

This is an Open Access document downloaded from ORCA, Cardiff University's institutional repository: <https://orca.cardiff.ac.uk/id/eprint/76441/>

This is the author's version of a work that was submitted to / accepted for publication.

Citation for final published version:

Mitchell, Neil, Simmons, Harper and Lear, Caroline Helen 2015. Modern and ancient hiatuses in the pelagic caps of Pacific guyots and seamounts and internal tides. *Geosphere* 11 (5) , pp. 1590-1606.
10.1130/GES00999.1

Publishers page: <http://dx.doi.org/10.1130/GES00999.1>

Please note:

Changes made as a result of publishing processes such as copy-editing, formatting and page numbers may not be reflected in this version. For the definitive version of this publication, please refer to the published source. You are advised to consult the publisher's version if you wish to cite this paper.

This version is being made available in accordance with publisher policies. See <http://orca.cf.ac.uk/policies.html> for usage policies. Copyright and moral rights for publications made available in ORCA are retained by the copyright holders.



Modern and ancient hiatuses in the pelagic caps of Pacific guyots and seamounts and internal tides

Neil C. Mitchell¹, Harper L. Simmons² and Caroline H. Lear³

¹School of Earth, Atmospheric and Environmental Sciences, University of Manchester,
Manchester M13 9PL, UK

²School of Fisheries and Ocean Sciences, University of Alaska-Fairbanks, 905 N.
Koyukuk Drive, 129 O'Neill Building, Fairbanks, AK 99775, USA

³School of Earth and Ocean Sciences, Cardiff University, Main Building, Park Place,
Cardiff CF10 3AT, UK

This is an open access version of an article published in *Geosphere* in 2015:

<http://www.crossref.org/iPage?doi=10.1130%2FGES00999.1>

Keywords: internal tides, guyot pelagic caps, pelagic sediment erosion, Pacific plate
tectonics

Abstract

Incidences of non-deposition or erosion at the modern seabed and hiatuses within the pelagic caps of guyots and seamounts are evaluated along with paleo-temperature and physiographic information to speculate on the character of Late Cenozoic internal tidal

waves in the upper Pacific Ocean. Drill core and seismic reflection data are used to classify sediment at the drill sites as having been either accumulating or eroding/non-depositing in the recent geological past. When those classified sites are compared against predictions of a numerical model of the modern internal tidal wave field (Simmons, 2008), the sites accumulating particles over the past few million years are found to lie away from beams of the modeled internal tide, while those that have not been accumulating are in internal tide beams. Given the correspondence to the modern internal wave field, we examine whether internal tides can explain ancient hiatuses at the drill sites. For example, Late Cenozoic pelagic caps on guyots among the Marshall Islands contain two hiatuses of broadly similar age, but the dates of the first pelagic sediments deposited following each hiatus do not correlate between guyots, suggesting that they originate not from ocean chemical changes but from physical processes, such as erosion by internal tidal waves. We investigate how changing conditions such as ocean temperature and basin physiography may have affected internal tides through the Cenozoic. Allowing for subsequent rotation or uplift by plate tectonics, ancient submarine ridges among the Solomon, Bonin and Marianas Island chains may have been responsible for some sediment hiatuses at these distant guyot sites.

Introduction

Within the subject of paleoceanography, much effort has been expended investigating the ocean structure of large-scale currents from paleontological, isotopic and geochemical evidence. Much less is known about water movements of shorter periods, such as associated with eddies, barotropic tides, internal waves and surface waves, although these

movements may have been significantly different in the geological past, for example, because wind and temperature regimes and physiography of the oceans and landmasses were different. Furthermore, the maximum current is commonly more important locally than the mean current for re-suspension and transport of particles and thus for influencing the sedimentary record. The amplitudes of current oscillations should therefore be of interest to paleoceanography, though are unfortunately poorly known for the geological past.

Hiatuses in pelagic sediments of the deep abyssal ocean floor have been interpreted from sediment cores (Barron and Keller, 1982; Keller and Barron, 1983; Moore et al., 1978). Hiatuses are formed by either physical removal of material by currents or dissolution of soluble components of the sediment. They can be difficult to recognize, being complicated by incomplete recovery of stratigraphy by coring and requiring missing biostratigraphic zones to be identified (Moore et al., 1978). In the study here, for pragmatic reasons we use low accumulation rates (condensed sections) as signs of breaks in sedimentation, which are loosely referred to as hiatuses, although they may not strictly speaking be hiatuses in the sense originally intended. Individual hiatuses have been attributed to changes in deep-ocean circulation originating from tectonic changes of gateways and changes in production of deep water at high latitudes (Barron and Keller, 1982; Keller and Barron, 1983). The presence of microfossils out of stratigraphic sequence is evidence that hiatuses can be at least partly caused by physical movements (Thiede, 1981). Barron and Keller (1982) noted that Miocene hiatuses correlate with sea-level lowerings, greater ^{18}O in benthic foraminifera and cool faunal assemblages, consistent with intensified deep-water production and circulation. However, Moore

(2013) argued that the general circulation was likely too sluggish to explain reworked radiolaria around the Eocene/Oligocene boundary in deep-water samples, suggesting that higher frequency motions such as from internal waves may have been involved.

The sediments deposited in the summits of guyots and seamounts potentially record changing physical conditions within the upper ocean. Watkins et al. (1995) noticed that pelagic cap thicknesses on guyots decline going north from the equator, diminishing to zero at around 25°N, a trend also found in seismic data (van Waasbergen and Winterer, 1993). Watkins et al. (1995) identified erosion as the cause of the thinning, although the origin of the erosion was unknown at that time. Pearson (1995) developed a higher resolution biostratigraphy of samples from three drill sites on guyots among the Marshall Islands. He identified hiatuses and noted that they terminated at different times, hinting that they had a physical rather than chemical origin. He suggested that pelagic cap development proceeds from an early barren stage to first accumulation under the influence of currents, allowing sediments to accumulate only in the center of the platform, followed by progressive expansion of that deposit to the platform edges under more quiescent conditions.

Increasing sophistication of physical oceanographic models, combined with more accurate estimates of basin shape (Smith and Sandwell, 1997) and ocean density structure, have allowed increasingly more accurate estimates to be made of physical conditions at the modern seabed. In addition, the GeoMapApp software tool (www.geomapapp.org) has provided easy access to a revised consistent stratigraphy of the drill cores recovered under the Deep Sea Drilling Project (DSDP) and Ocean Drilling Program (ODP) (Figure 1). This combination now allows an exploration of the spatial

correspondence between internal tidal wave propagation across the Pacific predicted by numerical modeling (Simmons, 2008) (Figure 2) with modern seabed hiatuses. Although the model and the geologic data represent markedly different timescales, we suggest reasons below why the internal wave field may not have changed greatly over the last few million years. Furthermore, assessing the presence or absence of hiatuses using seismic and drill core data together effectively provides estimates over large spatial and temporal scales, which can be preferable to overcome local variability likely to affect individual shallow cores. Given the modern correspondence, we then speculate on earlier conditions in the Late Cenozoic upper ocean. Although it is strictly speaking not possible to infer the ancient pattern of the internal wave field from the limited sedimentary information, we highlight some tectonic movements that potentially affected the wave field and might explain some hiatuses.

This issue is complex, so we devote the following section to describing the nature of internal waves (how they are generated and propagate) and other flow phenomena over seamounts and guyots, which may also affect sediment deposits. We then introduce the datasets and provide an interpretation of them, bearing in mind the physical oceanographic results. In the discussion, the origins of the earlier hiatuses are considered speculatively in terms of evidence for changing water temperatures and changing basin physiography, which affected the conversion of barotropic tides into internal waves.

Background

Internal tidal waves

Observations and modeling have improved understanding of internal waves over the

last decade. When tidal currents cross submarine ridges they excite oscillations (internal tides - internal waves at the barotropic tide frequency) in the density gradient of the upper ocean (pycnocline). The resulting energy transfer from the M_2 barotropic tide into internal waves is significant in the Pacific Ocean where tidal currents cross major ridges, in particular the Hawaiian Ridge, Tuamotu Archipelago (Tahiti), Aleutians and Izu-Bonin Arc (Egbert and Ray, 2003).

Based on numerical modeling and observations, internal tides propagate away from major topographic features such as the Hawaiian Ridge, forming beams in plan-view (Holloway and Merrifield, 2003; Merrifield et al., 2001). The waves have been revealed from satellite altimetry to radiate thousands of km from the Hawaiian Ridge and the Aleutians (Ray and Cartwright, 2001), but even these long distances may be underestimates because the altimetric method only detects waves that are in phase with the barotropic tide. More direct measurements from moorings and ships show internal tides can continue farther with remarkably little loss of power (Alford, 2003; Alford et al., 2007; Zhao et al., 2010), reaching 2400 km in one locality (Alford and Zhao, 2007). The altimeter data and modeling suggest that the Hawaiian Ridge currently generates internal tides from near Oahu to as far west as 175°W (Ray and Cartwright, 2001). A second type of internal wave, near-inertial internal waves, are generated from wind stress on the ocean surface, however, as the main generation sites are above 30° latitude and are typically surface intensified (Alford, 2003), they are less important than the tidal internal waves to our study.

Numerical modeling by Holloway and Merrifield (1999) investigated how internal tides are generated. For density stratification typical of the ocean around Hawai'i, the

models showed that wave energy flux 500 km from a ridge is insensitive to ridge depth when varying its depth down to 500 m, but energy flux declines by 25% when its depth is 1000 m. In contrast, isolated seamounts were found to be much weaker generators of internal tides by an order of magnitude in energy flux because the tide can pass around as well as over them. Further modeling using idealized seamounts has revealed how internal tides are scattered by topography in their paths (Johnston and Merrifield, 2003), complicating intensities in far-field sites. Ridges in the paths of the waves can lead to convergence or divergence of wave fluxes behind them, and can reflect energy if the internal tidal wave is supercritical with the bed, i.e., where bed gradient α is steeper than the wave characteristic gradient, c :

$$c = \left(\frac{\sigma^2 - f^2}{N^2 - \sigma^2} \right)^{1/2} \quad (1)$$

where σ is the internal wave frequency, f is the local inertial frequency and N is the Brunt-Vaisala frequency (Wunsch, 1969). For internal semi-diurnal tidal waves, $\sigma = 0.081$ cycles per hour (cph) and $f = 2 \Omega \sin(\phi) \text{ s}^{-1}$, where ϕ is latitude (degrees) $\Omega = 7.2921 \times 10^{-5} \text{ rad/s}$ is the rotation rate of the earth and N is (Gill 1982):

$$N = \left(\frac{g}{\rho_0} \frac{\partial \rho}{\partial z} \right)^{0.5} \quad (1a),$$

where g is the acceleration due to gravity (9.8 m s^{-2}) and ρ_0 is a reference fluid density, $\partial \rho / \partial z$ is density gradient at the depth of interest and z is depth. The parameter ρ represents potential density at a given depth in the oceans from local salinity and temperature (Gill 1982).

Figure 2 shows part of a global model of internal tide flux (Simmons, 2008). The

model depth grid was computed using a bathymetry dataset compiled using the marine gravity field estimated from satellite altimetry data to interpolate between soundings (Smith and Sandwell, 1997) and forced by a specified equilibrium tidal potential. The model grid is somewhat smoother than actual bathymetry in places and some generation sites may be weaker than in reality. The model also has rather crude representation of energy loss that may result in misrepresentation of internal tide energy levels.

Nevertheless, the results show sites of known internal tide generation highlighted (circles) in Figure 2, including the French Frigate Shoals and Kaena Ridge in the Hawaiian islands. Other important sites are ridges underlying the Kuril, Aleutian, Bonin and Mariana Islands and a gap between Bougainville and New Ireland where the barotropic tide exchanges between the Solomon Sea and the Pacific Ocean.

Sediment erosion thresholds

To evaluate the importance of the current magnitudes below, it is useful to be aware of re-suspension thresholds for pelagic sediments. Unless winnowed by currents, carbonate pelagic sediments typically found on guyot summits contain nannofossils and foraminifera. Their grain sizes range from clay to sand, usually dominated by clay and silt sizes by mass (e.g., Leg 55 Scientific Staff, 1980). Aside from organic components usually removed by oxidation, the primary input of particles falling from surface waters is expected to have this wide particle size range. Also because particles have low densities due to calcite or aragonite compositions and porous structures, they are susceptible to erosion by currents. Critical erosion thresholds measured in laboratory experiments range from 7-10 cm s^{-1} for freshly deposited calcareous material to 15-20 cm

s^{-1} after being deposited a few hours in a flow 5-6 cm deep (Southard et al., 1971) (the experimental 10 and 20 cm s^{-1} is equivalent to 18 and 36 cm s^{-1} at 1 m above bottom when corrected for the boundary layer effect). Phytodetritus has been found to have smaller erosion thresholds by around half or less (Beaulieu, 2003; Mitchell and Huthnance, 2013; Thomsen and Gust, 2000) compared with the Southard et al. (1971) values. Before degradation of organics, phytodetritus and associated inorganic particles may be susceptible to re-suspension by currents as small as 5 cm s^{-1} or less, allowing any embedded solid tests (microfossil skeletons) to be advected away.

Local flow patterns over seamounts and guyots

Turnewitsch et al. (2013) have summarized some of the various flow patterns found over seamounts. Rotational current patterns have been predicted and observed over seamounts and guyots (Lavelle and Mohn, 2010), which are relevant to the patterns of sediment deposition in the seismic data that we describe later. A steady current in a density-stratified ocean is predicted to produce a rotating body of water above seamount summits (Chapman and Haidvogel, 1992; Verron and Le Provost, 1985; Zhang and Boyer, 1991) (the so-called "Taylor cap" after Taylor (1923)). Simulations show semi-diurnal tidal currents amplified where they interact with seamounts (Beckmann and Haidvogel, 1997). Other simulations show how seamounts can produce lee-side eddies when impacted by steady currents (Zhang and Boyer, 1991).

Above Fieberling Guyot in the subtropical NE Pacific (where the summit shoals above 500 m depth), weak radial currents but significant azimuthal mean currents increasing to 10 cm s^{-1} at the summit rim have been observed (Brink, 1995; Kunze and Toole, 1997).

A similar rotational current pattern with order 10 cm s^{-1} speeds has been found above Cobb Seamount farther north in the NE Pacific (summit reaching to only 24 m below sea level) (Codiga and Eriksen, 1997; Freeland, 1994), with semi-diurnal currents reaching $20\text{-}40 \text{ cm s}^{-1}$ (Eriksen, 1991). Current fields with a rotational component have been observed on other seamounts (Mohn et al., 2009; Mouriño et al., 2001) and inferred in sediment geochemical data (Turnewitsch et al., 2004). A drifter experiment around the Emperor Seamounts discovered eddies attached on one side of the seamounts, with movements of $20\text{-}40 \text{ cm s}^{-1}$ at 120 m depth (Bograd et al., 1997). These various motions typically involve intensified flow near the summit margins of the seamounts or guyots with speeds that are comparable with the suspension thresholds of pelagic sediments and thus can be expected to lead to thin deposits or bare rock towards the summit margins.

Oceanographic and geological observations on Horizon Guyot

Studies of Horizon Guyot are useful for illustrating the sedimentary effects of internal tidal waves. The guyot is an east-northeast to west-southwest oriented ridge that was sampled by the DSDP. Figure 3 shows an interpretation of a seismic record through Site 44 (Shipboard Scientific Party, 1971), suggesting erosional truncation of strata at the seabed. This pattern of erosion around the sides of the sedimentary cap is as would be expected from the kinds of rotational flows described earlier. Recovered shallow cores contain mostly fine to medium foraminiferal sand of Eocene and Quaternary particles (Lonsdale et al., 1972; Schwab et al., 1988), produced by removal of finer particles by current winnowing. Sediment bedload movements are suggested by the presence of current ripples and dunes in bottom photographs and high-resolution sonar images

(Lonsdale et al., 1972). Schwab et al. (1988) and Kayen et al. (1989) assessed slope stability using geotechnical parameters measured from cores to infer that shallow slumping (a further cause of erosion) is possible on the pelagic cap during shaking by rare earthquakes, particularly if internal wave activity has over-consolidated surface sediments while leaving underlying sediments normally consolidated. Slumping could also be promoted by the undermining of the edges of the sediment cap by currents.

Current and temperature data obtained from a 9-month mooring deployment 213 m over the summit recorded internal tides (Cacchione et al., 1988; Noble et al., 1988). Those data revealed 15-18 cm s⁻¹ peak semi-diurnal currents and 15-20 cm s⁻¹ peak low-frequency flows occurring during spring, which Cacchione et al. (1988) showed together could exceed the threshold of motion of the bed sediments. From the phase of the currents compared with the surface (barotropic) tide, the currents were shown to be locally generated internal tidal wave currents.

Data compilation

Seismic reflection and scientific drilling data were compiled for guyot or seamount pelagic caps in the central and western Pacific (Figure 1). Scientists from Columbia University have revised the absolute age data of DSDP and ODP site stratigraphy available within the GeoMappApp software (WBF Ryan, pers. comm., 2009; www.geomapp.org) (Gradstein and Ogg, 2004). Those ages are plotted along with depth below seabed in Figure 4. Unfortunately, many of the sites were drilled close to the summit margins, where the onsets of pelagic sedimentation likely occurred later than the onsets in the pelagic cap centers. Furthermore, core recovery was limited in the early

stages of DSDP, so biostratigraphic resolution is likely to be non-uniform. Figure 4 is used only to gauge general trends.

Pearson (1995) developed a high-resolution biostratigraphy for ODP Sites 871, 872 and 873 on three guyots among the Marshall Islands. His dates are shown versus depth below seabed as small solid circles in Figure 5 (lower panel), along with his interpreted hiatus depths and other data for comparison.

The benthic $\delta^{18}\text{O}$ record contains both a salinity and temperature signal, so estimates of deep ocean temperatures are instead based here on Mg/Ca ratios of benthic foraminifera. Grey squares in Figures 5 and 6 (top graphs) represent estimates of global temperatures derived from deep-sea sites (Lear et al., 2000). Discrepancies between sea surface paleotemperature proxies have been attributed in part to recrystallization of calcite foraminiferal tests, making $\delta^{18}\text{O}$ -based temperature estimates unreliable (Pearson et al., 2001). Pearson and co-workers (Pearson et al., 2001; Pearson et al., 2007; Stewart et al., 2004) have argued that pelagic foraminifera recovered from impermeable shales in Tanzania are sufficiently well preserved that original compositions can be extracted from them. Those data are displayed with various symbols in Figures 5 and 6 as described in the figure caption to Figure 6.

Seismic and sediment profiler records were extracted from the ODP reports. A selection was chosen where sites were drilled away from summit margins and where high-resolution stratigraphy data were available. Figure 7 shows three seismic profiles crossing Allison Guyot (ODP Site 865) and Figure 8 shows profiles crossing Wodejebato, Lo-En and Limalok Guyots (sources given in figure captions).

Figure 9 shows temperature-depth profiles (upper graphs) from CTD deployments

over Allison, Horizon, Limalok, Lo-En and Wodegebato guyots, as well as on the equator (accessed through the GeoMapApp data portal). Seawater potential densities were computed from these values using the procedure in Joint Panel on Oceanographic Tables and Standards (1991) and are shown in the lower graphs in Figure 9. From the mean density and density gradient with depth of each profile at the depth of the drill sites, the characteristic gradient (c) of internal semi-diurnal waves was computed using Equation (1). Those values given on Figures 3, 7 and 8 are almost uniform between sites due to the uniformity of ocean temperature in the tropics and similar depths of the guyot summits. In most of the cases, c is smaller than the gradients of the pelagic cap sides shown on the figures, so internal waves, if present, are likely to break and intensify (Cacchione and Drake, 1986; Cacchione et al., 2002) as waves pass from the slopes to the summit. For comparison, Cacchione et al. (1988) estimated a modestly different $c=0.085$ for Horizon Guyot.

Observations

Depth-age graphs (Figures 4 and 5)

The low-latitude Sites 871-873, 202, 200 and 171 show recent steady accumulation but low sedimentation rates in earlier periods (Figure 4). Some other sites show low sedimentation rates at the seabed but earlier periods of more steady accumulation, such as Sites 865, 44 and 866. Of the latter, Site 866 unfortunately lies close to a summit margin and 171 lies within a topographic saddle so they are not considered further.

Of the Emperor seamount sites, many unfortunately also lie close to summit margins (1206, 308, 1205, 432). Of the remainder, Site 430 shows no significant recent

accumulation whereas 433 shows a 10-m.y. period of recent accumulation following a long period of slow accumulation. The pelagic interval in the Detroit Seamount sites lies beneath a sediment drift, whose lower boundary is marked by dashed lines in Figure 4. Prior to drift sedimentation, pelagic sediments accumulated following a barren stage.

These data appear generally to record an initial period of very slow deposition or non-deposition, followed by a period of intermittent pelagic accumulation. The onset of the pelagic stage was interpreted from these data, referring to the drilling reports. The onset dates plotted in the middle graph in Figure 6 ('x' symbols) show no obvious correlation with other parameters, such as phases of changing sea level or paleo-temperature.

In the data of Pearson (1995) shown in Figure 5, the onsets of pelagic accumulation following hiatuses (circled) have different dates in the three sites. Three periods occur where hiatuses apparently overlapped in time between the three sites (at 8, 14 and 24 Ma), although in practice we cannot be sure that intervening deposits have not been removed by the erosion so we concentrate more on the accumulation onset dates following each hiatus. As noted by Pearson (1995), the onset dates do not correspond between the sites. The hiatus termination at 5 Ma at Site 873 lags that at 872 by about 2 m.y., whereas, while there is a similar termination age at 871 to that at 872, the 871 record has two further small hiatuses until steady accumulation resumed at 2 Ma. The next-oldest hiatuses terminated around 13 Ma at 873, 15 Ma at 872 and 13 Ma at 871. Hiatuses at 872 and 871 also occur at around 20 Ma but the weaker biostratigraphic age constraints at 871 may have made identification of hiatuses difficult in this part of the section.

Between these hiatuses, the sediments are winnowed foraminiferal oozes with

foraminifers accounting for up to 90% and some microfossils out of stratigraphic sequence (Watkins et al., 1995), in contrast to the Pliocene and Quaternary sediments above the last hiatus, which are nannofossil oozes. A tendency for foraminifers to be more resistant to erosion has been confirmed in laboratory experiments (Black et al., 2003). The lower-right graphs in Figure 5 suggest that the transition from coarse particles towards around 60% sand or foraminifers at the modern seabed occurred gradually at Site 872 since the last hiatus. Because of incomplete data in the 871 record, the transition there cannot be interpreted but it nevertheless also shows a change to finer sediment towards the seabed. Although smear slide data are often considered only rough indicators of sediment composition because of effects of dissolution, test fragmentation and interpreter bias, these trends seem clear and the analyses were carried out during a single drilling expedition.

Figure 6 (solid circles in middle graph) shows the pelagic onset depths compensated for subsidence. To compute these depths, we found subsidence relationships (Detrick and Crough, 1978) unreliable so only sites where an age of drowning of the platform is available were used, allowing the depth of initial sedimentation to be estimated by interpolation. Three of the sites shown are from Pearson (1995). Reef limestone growth at Site 433 on Suiko Seamount (McKenzie et al., 1980) terminated in the lower Eocene on the basis of nannofossils (Koizumi et al., 1980) (biostratigraphic zones NP 7 to 10) and is assigned a date of 50 Ma in the GeoMapApp database. According to Winterer et al. (1995), the limestone platform of Allison Guyot emerged above sea level and subsequently drowned post-Albian but before mid-Turonian. Within the GeoMapApp database, an age of 100 Ma has been assigned. We have used that date and 93 Ma (the

Turonian/Cenomanian boundary) to represent a possible range of drowning times. With these data, the reconstructed depths of onset of pelagic sedimentation are 753-816 m (Allison) and 1430 m (Suiko). The average onset depth of all five sites is 928 m.

Unfortunately, the remaining sites had ambiguous evidence of shallow water deposits and hence drowning ages (two sites are therefore shown merely with modern depths).

Seismic and profiler records

In Figure 7a (Allison Guyot), seismic reflections lying roughly horizontal within the upper part of the section appear truncated where they reach the seabed and the seabed reflection has a slightly stepped structure, as would be expected for erosion of strata of varied geotechnical properties and hence resistance to erosion. In Figures 7b and 7c, the reflections within the pelagic cap are somewhat convex-upwards but still terminate at the seabed and the seabed reflection in Figure 7c is also slightly stepped. Winterer and co-workers (Winterer and Sager, 1995; Winterer et al., 1995) interpreted these sequences as pelagic sediments overlying an atoll or karstic limestone basement. A small collapse structure typical of karst topography can be observed on the left of Figure 7c. The very low sedimentation rates for the past 20 m.y. in Figure 4 for Site 865 correspond with apparent seabed erosional evidence in these seismic data.

In Figure 8a (Wodejebato Guyot), the seabed forms a low relief but smooth surface. Internal reflections are difficult to interpret from this profile but a thin layer is consistent with only ~50 m of pelagic sediment recovered at Site 873 (Figure 5).

In Figure 8b (Lo-En Guyot), the seabed to a few 10s of ms comprises laminated sediment with reflections sub-parallel to the seabed. Below that, a series of reflections

can be observed dipping down from right to left in the profile. The boundary between these two sets of reflections is not visible but is suspected to be an unconformity. The depth of the youngest hiatus in the analysis of Pearson (1995) is marked by the topmost red bar, which almost corresponds to the proposed unconformity. Similar features are observed in the seismic data in Figure 8c, although the irregular reflection observed just above the top red bar in Figure 8b is not visible.

In Figure 8d (Limalok Guyot), near-surface reflections also lie sub-parallel with the seabed. Below the near-surface reflections, the section is more transparent (lacking reflections) down to a prominent reflection about 200 ms below the seabed. Although discordant reflections cannot be interpreted here, the base of the near-surface reflections approximately corresponds with the first hiatus of Pearson (1995). A mound-like feature is observed within the otherwise transparent sediments south of Site 871.

Interpretations

Spatial patterns of erosion or deposition and currents above the seamounts and guyots

The profile shapes of the pelagic caps and near-surface stratigraphy partly reflect how accumulation rates of the clay and silt size components of primary input have been modulated by the currents (spatial variations in the vertical spacings of reflectors indicate how time-averaged accumulation rates have varied spatially). McCave and Swift (1976) showed how an earlier empirically determined relation for fine particle accumulation rates (Odd and Owen, 1972) was compatible with a model in which accumulation was dictated by capture of particles within a viscous boundary layer. The data predict the instantaneous accumulation rate R :

$$R = Cw_s \left(\frac{\tau_l - \tau_0}{\tau_l} \right) \quad (2),$$

where C is the mass concentration in the bottom waters, w_s is the particle settling velocity for a particular grain size component, τ_0 is the bed shear stress due to the current and τ_l is a limiting stress above which no deposition occurs (increasing with grain size and w_s). Although current intermittency and various effects modulating resistance to resuspension are also important (McCave, 1984), the shapes of the near-surface reflection spacings should broadly follow how the currents have modulated the bed shear stress τ_0 and thus R in a time-averaged sense. Grain size and other data are generally lacking so quantitative interpretation of those spacings is not possible. However, given that R is proportional to $(\tau_l - \tau_0)$ in Equation (2) and as τ_0 is proportional to the current squared ($\tau_0 \propto u^2$), the patterns of time-averaged deposition rates should indicate where u has been small in a time-averaged sense, provided that C and the other factors in equation (2) have not varied greatly over these structures. Thus, the reflections in Figures 8b and 8d paralleling the seabed suggest that these sites have recently experienced conditions that were uniform as well as quiescent. The dipping reflections in the lower part of the pelagic cap in Figure 8b imply deposition under a current with a strong unidirectional component producing asymmetric bed shear stress. In contrast, the package of reflections in the uppermost 30-40 ms of reflective stratigraphy in Figure 8b thins modestly to the SE, suggesting that the unidirectional component has reversed direction. Erosion occurs when stresses rise above a threshold (McCave, 1984), so the truncation of reflections around the margins of Allison and Horizon Guyots (Figures 3 and 7) imply greater current stresses around the sides of the caps than over their summits, consistent with strong rotational components to

the current fields there.

A gravity effect on cyclically agitated bedload particles can lead to a small down-gradient flux, which, combined with considerations of continuity, produces a diffusion of the seabed topography if it acts alone (Mitchell and Huthnance, 2007). As the bed gradients of the guyot caps are small (Figures 7 and 8) and the primary input is mostly finer than sand grade, this mechanism is unlikely to dominate, though the upward-convex shapes of the sediment caps are similar to the parabolas expected of steady state solutions to the diffusion equation for this geometry and boundary conditions (Mitchell, 1995). Gravity effects on bedload may be important around summit margins where gradients are steeper and where the sediment has been strongly winnowed leaving mainly sand.

Relationships to the modern internal wave field

Ten sites (larger symbols in Figure 2) were deemed sufficiently well characterized to allow them to be classified as having been either accumulating sediment particles or non-depositing / eroding in the past few million years. The pelagic cap around Site 44 has already been shown to be the latter (Cacchione et al., 1988; Lonsdale et al., 1972). Also eroding or non-depositing are Allison Guyot, indicated by its seabed unconformity (Figure 7), and Ojin Seamount, where drilling to 14 mbsf (metres below seafloor) recovered only pebbly mudstone including Recent to Eocene shallow-water fossils (Shipboard Scientific Party, 1977a). The seismic data collected over Ojin were of poor quality but appear to rule out a thick, draping pelagic cap. The first three cores recovered at Site 865 on Allison Guyot contained winnowed foraminiferal sand (Shipboard Scientific Party, 1993a), suggesting a recently energetic environment. A pelagic section

to 3.2 mbsf was sampled at Site 878 on MIT Guyot and includes nannofossils (Shipboard Scientific Party, 1993c). However, the limited thickness of this unit and the lack of pelagic sediment visible in the seismic and 3.5 kHz profiler data collected over the guyot summit led us to classify this site as generally non-depositing. Site 866 was drilled 1.5 km from the edge of Resolution Guyot (Shipboard Scientific Party, 1993b). Pelagic sediment thicknesses of only 0.9 m at 866A but 23.5 m at 866B were found, extending in age to Maastrichtian. The 3.5 kHz profiler data show a transparent unit ~40 ms thick (~30 m) at Site 866, thinning into the platform. The drilling report mentions only a thin pelagic cover. We classify this as weakly sedimented and report it separately from the other two classifications.

The accumulating sites include Wodegebato, Lo–En and Limalok guyots on the basis of seabed–following seismic reflections in the latter two sites and the stratigraphy in Figure 5 being relatively continuous towards the seabed. Suiko Seamount was also classified as accumulating on the basis of its depth–age graph (Figure 4) and of >50 m of Recent to Miocene pelagic sediments recovered (Shipboard Scientific Party, 1977b). The seismic data published in the Site 433 drilling report suggest pelagic sediments overlie a lagoonal complex, possibly within a graben structure, but have been accumulating asymmetrically, suggesting possible influence of a steady current on the seamount. This site is less convincing than the others classified as accumulating. Site 200 was drilled somewhat near the summit margin of Ita Mai Tai Guyot, but nevertheless the presence of thick sediments in seismic data across the summit and the lack of truncation of strata at the seabed show that it has been accumulating (Shipboard Scientific Party, 1973) and this has continued recently (Figure 4). According to the site report, the sediments here

include winnowed foraminiferal ooze, so this site is not as quiescent as some of those in the Marshall Islands.

Although the timescales of deposition above are long compared with those of many physical oceanographic processes, conditions have probably not changed greatly in the past few million years for reasons we outline later. Modeling by Egbert et al. (2004), for example, shows little change in the Pacific barotropic tide between the present day and the Last Glacial Maximum (LGM) when sea level was much lower. The classified sites are plotted in Figure 2 over the modern internal wave field of Simmons (2008), with unfilled circles for accumulating sites and filled circles eroding for non-depositing sites. Despite the irregularities in the computed wave field, the accumulating guyots in the Marshall Islands (Ita Mai Tai, Wodejebato, Lo-En and Limalok) all lie away from the beams of internal wave energy emanating from the Mariana Islands and Solomon Sea-Pacific gateway. Of the eroding / non-depositing sites, Allison arguably lies on crossing long-range beams originating from the Bonin Islands and Hawaiian Islands. Horizon does not appear to be on a beam of propagated wave energy but is known to experience locally generated waves (Cacchione et al., 1988; Noble et al., 1988). Resolution lies within waves originating from the Bonin Islands but was marginally classified as accumulating. Suiko and Ojin seamounts less obviously relate to internal wave beams.

The internal wave model results were sampled at the site locations. All eroding / non-depositing sites were found to be separated from all depositing sites by a kinetic energy flux magnitude of 10^3 W m^{-1} . Although that separation may not be so significant given irregularities in the model and some site classification issues, their mean values are markedly different, 544 and 1924 W m^{-1} for depositing and eroding sites, respectively.

The value for the Resolution Guyot site is anomalous at 2513 W m^{-1} . Nevertheless, aside from that site, the pattern of erosion and deposition on the sediment caps appears compatible with the modern internal tidal field despite the different timescales represented by the data and model.

Discussion - origins of the older hiatuses

Prior to carrying out this analysis, the incidence of erosion / non-deposition and accumulation was anticipated not to correspond exactly to the internal wave field because of the other types of currents that can occur in the mid-ocean. However, for the pelagic caps studied here, internal waves seem to be important for elevating bed stress above the erosion threshold. In the light of this, the origins of hiatuses lower in the stratigraphy are considered. The youngest sediment immediately overlying each hiatus in Figure 6 varies in age between the sites, a strong clue that the hiatuses had a physical, rather than chemical origin, which would likely be more synchronous. We however first evaluate some circumstantial evidence for chemical origins.

Hiatuses appear throughout the Late Cenozoic stratigraphy of the abyssal Pacific Ocean sediments (Barron and Keller, 1982; Keller and Barron, 1983; Moore et al., 1978). The central ages of the hiatuses identified by Keller and Barron (1983) were updated to the timescale used within GeoMapApp (Gradstein and Ogg, 2004) and are shown by vertical bars in the lower graph of Figure 5 (NH7, etc). No particular correspondence is observed with the guyot hiatuses. Ujiie (1984) attributed one abyssal hiatus to meso-scale eddies, which typically occur with ocean boundary currents. Many of the sites examined here are away from boundary currents, however. The northwards drift of the

Pacific tectonic plate has been $\sim 0.25^\circ$ of latitude m.y.^{-1} for the past 40 m.y. (Mitchell, 1998) so the Marshall Islands guyots presently lying at 5.6° - 11.9°N lay at the equator at 22-48 Ma. Measurements with current meters have recorded flows of 10 - 20 cm s^{-1} at 300 m depth at 4°N (Hayes et al., 1983), 40 cm s^{-1} at ~ 1000 m depth at 1°N , 150°W (Taft et al., 1974) and a standard deviation of zonal current of 10 cm s^{-1} at 900 m depth at the equator at 159°W (Firing, 1987). These currents are sufficient to re-suspend silt grain sizes and, if present prior to 20 Ma, equatorial currents may help to explain the delayed start of pelagic accumulation on the Marshall Island guyot summits (Sites 871-873) compared with Allison and Horizon, for example (Figure 4). The sequence of onsets is not simply as expected from equatorial provenance because the northernmost of the Marshall Island sites, Wodejebato, started accumulating later (Figure 6) rather than earlier as might be expected given its latitude. Nevertheless, the onsets of Ita Mai Tai, Lo-En and Limalok are in the correct order for this interpretation.

The occurrences of pelagic cap hiatuses are compared with the carbonate compensation depth (CCD) in Figure 5 because, although the CCD lay persistently deeper than the pelagic caps, the lysocline (dissolution gradient) extends perhaps ~ 2000 m shallower than the CCD (Berger et al., 1976) and waters at 1000 m depth are under-saturated with respect to carbonate (Peterson, 1966). Although the onset dates of hiatuses are uncertain due to erosion (so we cannot rule out chemical erosion caused by the shoaling of the CCD playing a role at 10 Ma), the terminations of the hiatuses are not associated with CCD deepening. Furthermore, the earlier two major hiatus terminations phases do not correspond with CCD deepenings. The lack of correlation is consistent with the view that carbonate loss above the lysocline arises mainly from oxidation of

organic matter (Peterson and Prell, 1985), which depends on the organic to inorganic carbon ratio of the sediment input and may not be related to the CCD.

Further work on carbonate saturation state based on Li/Ca and Mg/Ca ratios of benthic foraminera corroborate these observations of CCD shifts. The foramineral Li/Ca ratio has been shown to vary with carbonate saturation state (carbonate ion concentration relative to concentration expected at saturation) in modern environments (Lear et al., 2010; Lear and Rosenthal, 2006) and a model-based calculation can be carried out with the aid of Mg/Ca ratios to estimate past carbonate saturation states. Li/Ca ratios from the equatorial Pacific show no obvious shift at the time of the terminations of the younger (8-10 Ma) hiatuses in Figure 5 (Lear and Rosenthal, 2006). Saturation states computed from data over the period corresponding with the earlier hiatus show a general peak in saturation rather than trough around 15 Ma, corresponding to the middle hiatus phase (Lear et al., 2010).

Although chemical effects may have played some roles in developing these hiatuses, physical effects seem more likely to have dominated. The declining thickness of sediment caps going north of the equator noted by Watkins et al. (1995) can be explained by the migration of sites across successive internal tidal wave beams as they migrated northwards (Figure 2). We attempt below to identify possible changes affecting the Cenozoic ocean that could explain the varying pattern of accumulation, in particular on the Marshall Islands guyots.

Ocean tides and sea level

To address whether internal tides were different in the past, the forcing by barotropic

tides also needs to be considered, though they are poorly known further back in the Cenozoic. The power acquired by the modern tide from the Moon and Sun is mainly dissipated by friction in the shallow waters of continental shelves. Modeling by Egbert et al. (2004) suggests that the deep-water Atlantic tidal range was in places twice as large during the Last Glacial Maximum as during the present day because dissipation on the shelves was smaller when coastlines had extended seawards with a lower sea level. This variable dissipation effect was more limited in the Pacific where continental shelves are narrower. A lack of amplification of the tide by sea-level lowerings has probably persisted for much of the Cenozoic because subduction zones (regions that are tectonically mobile and hence unlikely to develop wide shelves through coastal erosion) have persistently ringed the basin. Prior to the Pleistocene, sea level variations were also smaller (from $\delta^{18}\text{O}$ in Figure 5), implying less varied shelf dissipation effect. Furthermore, there is no obvious correlation between sea level changes and the hiatus terminations in Figure 5. For example, if the terminations around 13-15 Ma at the three ODP sites were associated with sea level rise and a more attenuated tidal range, they should be accompanied by a decrease in $\delta^{18}\text{O}$, not the increase observed.

In the earlier Cenozoic, deep-water tides are more difficult to predict. Plate tectonic reconstructions show that the seaway between the American plates remained small (Meschede and Frisch, 1998), whereas others (Briden et al., 1981; Hilde et al., 1977) show a 3000-km-wide seaway between Australia and Indonesia progressively closed from 60 Ma to the present day. Tides in the Pacific may have therefore been influenced by the Indian Ocean tide, but overall there seems unlikely to have been larger amplitude or more variable tides in the past.

Changes in ocean temperature structure

Estimates of tropical paleotemperatures of the ocean surface and bed provide bounds on likely changes in the Pacific pycnocline. For the abyssal ocean, the Mg/Ca-based data in Figure 6 suggest a generally declining trend of $>10^{\circ}\text{C}$ over the past 50 Ma with stages of stasis. The surface ocean temperature data (Figures 5 and 6, upper graphs) have been more controversial. Zachos et al. (2002) suggested that the Eocene record for Tanzania may have been affected by a warm western boundary current and noted potential effects of its continental shelf location on salinity and ^{18}O . However, Pearson et al. (2002) argued that a salinity effect is likely to be only 2°C and that the site lay on a narrow shelf and steep margin. The paleotemperature data suggest surface waters declined by only a few degrees since 50 Ma, while benthic temperatures declined by $>10^{\circ}\text{C}$. Using a constant salinity of 35 ppt, seawater potential densities (ρ_{θ}) were calculated for temperatures of 32° and 27°C (50, 0 Ma, respectively) and deep water temperatures of 13° and 0°C using the equations of Joint Panel on Oceanographic Tables and Standards (1991). The resulting values (1021.0, 1022.7, 1026.4 and 1028.1 kg m^{-3} , respectively) suggest that the density difference due to temperature has remained a constant 5.4 kg m^{-3} to the present day.

The thermocline (vertical temperature gradient) of the upper ocean results mainly from advection of surface heat by turbulence created by surface wind stress (Apel, 1987). Changing wind stress through the Pleistocene implied by varying halite and dust in ice cores (Mayewski et al., 1994) suggests that there may have been varied upper ocean mixing. Farther back, however, there is evidence from organic proxies of sea surface

temperature that the inter-zonal air temperature gradients driving trade winds were less than half in the Early Eocene compared to today and strengthened progressively through the Middle Eocene (Bijl et al., 2009). Wind-driven mixing may therefore have been less efficient in the Early Eocene and the pycnocline may have been less steep at ~1000 m relevant to the early tops of the guyots (Figure 6), though we cannot know by how much. This also implies a smaller N and hence larger characteristic gradient c (equation (1)). Therefore, whereas the temperature difference between abyss and surface ocean implies relatively little change in the maximum density difference and hence effect on internal waves, wind stress changes may have made it somewhat less likely that breaking internal waves occurred on the guyot summits in the Eocene.

Plate tectonic motions and the changing internal wave field

The sills presently creating internal wave beams (Figure 2) lie around the Pacific basin (largely island arcs) and some within the basin (ocean island hotspot chains such as that forming the Hawaiian ridge). While it is difficult to reconstruct accurately the paleogeography of these areas, the depths of these sills are likely to have changed with tectonics of the subduction zones and with lithospheric thermal subsidence in the case of ocean island hotspot chains. Other wave-generating sills may have existed previously but have now been lost as seaways closed by tectonic uplift. Here we speculatively link tectonic changes with depositional changes within the guyot caps. The purpose is not to reconstruct the wave field but rather to highlight plausible origins of changes in the sediment record.

Solomon Sea-Pacific site

At present, the seaway between the Solomon Sea and Pacific Ocean extends down to ~1000 m north-northwest of Bougainville Island (Figure 1), creating a wide band of internal wave energy extending northeast (Figure 2), originating from the barotropic tide travelling from the Solomon Sea into the Pacific Ocean. Although the dating of vertical tectonic movements is too coarse and paleogeography too uncertain to explain individual hiatuses in Figure 5, known solid-earth movements within the Solomon Islands area are broadly coincident with some of the sedimentary changes in the Marshall Island guyots. Sites 871-873 have presently no island or shallow bank topography blocking potential internal waves arriving from the Solomon Islands and local physiography (Ryan et al., 2009) suggests they are open to waves from that direction.

The Solomon Islands lie above a subduction zone that switched sense from previously subducting the Pacific plate beneath the islands (then attached to Indo-Australia), to subducting the Indo-Australian plate beneath the islands (now attached to the Pacific plate). This change occurred prior to 6 Ma (Schuth et al., 2009) or at about 5 Ma (Mann and Taira, 2004). Based on the known geology of the islands and plate tectonic reconstructions of Mann and Taira (2004), we suggest the following possible paleo-generators of internal wave energy. Figure 10 shows how the relationship between the drill sites and the Solomon Islands changed since 8 Ma, based on the reconstructions.

First, an internal-wave generation site may have existed in the vicinity of Choiseul Island ("C" in Figure 10) where Pleistocene limestone is now found to 335 m above sea level (asl) (Coleman, 1962). The New Georgia Island Group ("NG") has been uplifted rapidly during the late Quaternary, locally up to 7.5 mm yr^{-1} , because of subduction of the

Woodlark Basin spreading center and associated seamounts (Crook and Taylor, 1994; Mann et al., 1998) and may not have existed to block propagation of the barotropic tide into the Pacific much earlier. Before the 335 m of Pleistocene uplift, the eastern third of Choiseul Island would probably have lain below sea level, with it and the adjacent seaway extending to Santa Isabel ("SI"), forming a sill at about 300 m depth. This feature lay roughly perpendicular to Sites 872 and 873.

Second, Malaita Island ("M") is an uplifted anticlinorium (Pettersen et al., 1999) or accretionary prism (Mann and Taira, 2004). A transition between open ocean pelagic carbonate rocks and higher-energy terrigenous clastic rocks occurs at 5.8 Ma (Musgrave, 1990). Guadalcanal Island ("G") has significant relief (2400 m asl) and is unlikely to have been below sea level during the late Cenozoic but late Cenozoic marine sedimentary rocks (Thompson and Hackman, 1969) nevertheless suggest that some uplift occurred. Thus, the seaway presently between Guadalcanal and Makira ("MA") marked by the lowermost dotted circle in Figure 10 would have been wider, with the eastern shelf of Guadalcanal deeper, forming a ridge potentially capable of generating internal waves. Interestingly, the 5.8 Ma date for the uplift of Malaita Island is similar to the hiatus termination dates of Sites 872 and 873.

Third, plate tectonic reconstructions show that Vanuatu Island ("V") and its associated banks have rotated clockwise and prior to about 8-10 Ma they were roughly co-linear with the Solomon Islands (Mann and Taira, 2004) (Figure 10). As ODP Sites 871-873 lay east of their present positions (relative to the Solomon Islands) by around 500 km at 10 Ma, these banks were roughly perpendicular to Site 871, potentially explaining the hiatuses prior to 13-15 Ma.

Mariana and Bonin ridges

The ridge on which the Mariana Islands lie originates beams of internal wave energy presently running southeast, just missing Ita Mai Tai and the other Marshall Islands guyots (Figure 2). Two main conversion sites occur at 14° and 16°N, where submarine banks or ridges lie roughly parallel to the arc at these latitudes. In plate tectonic reconstructions (McCabe, 1984; Uyeda and Miyahiro, 1974), the Mariana island arc has become progressively more convex eastwards and both it and the Bonin arc have rotated clockwise. If there were no change in incidences or depths of sills, this could have redirected internal wave energy clockwise. Guam and Saipan islands lie in the southern Marianas. Paleomagnetic measurements on igneous rocks on Guam (Larson et al., 1975) suggest 55° average rotation has occurred since the early Miocene. Similar results were obtained by Haston and Fuller (1991), who also reported clockwise rotations of Saipan, though of smaller magnitudes (Middle Miocene 28° and Eocene 43°). Clockwise rotations of 30°–90° or more have been documented in Eocene rocks of the Bonin Islands (Keating et al., 1983; Kodama, 1981; Kodama et al., 1983). The consistency of these rotations led Haston and Fuller (1991) to suggest that they occurred by rotation of the whole Philippine Plate rather than from local movements. Their reconstructions show the ridges lying 30° and 70° anti-clockwise of their present orientations at 10 and 30 Ma, respectively. If there were no change in sill depths and other factors causing internal wave generation, the internal wave beams from the Bonin Islands were pointed away from Allison Guyot at some point prior to 10 Ma and have since rotated towards it, helping to explain the declining accumulation rates followed by erosion (Figure 4).

Similarly, rotation of the Marianas wave beams so that they intersected the Marshall Islands guyots at some stage since 10 Ma may help to explain the hiatuses in Figure 5.

Complicating this interpretation, however, reef limestones of Miocene age on Guam and of Oligocene-Miocene age on Saipan (Haston and Fuller, 1991) are evidence that significant uplift has occurred locally and the sill configurations are unlikely to have been fixed. Geology of the Bonin Islands summarized by Haston and Fuller (1991) also includes subaqueous-erupted pillow lavas and hyaloclastites as well as pelagic sedimentary rocks, implying uplift.

Aleutian and Kuril Islands

The depth-age graph for DSDP Site 433 (Suiko Seamount) shows that pelagic sediment began accumulating only at 10 Ma, while Site 430 (Ojin Seamount) has remained barren. Attributing these changes to tectonic movements in Kiril and Aleutian arcs is difficult given the lack of information on those islands but nevertheless large rotations about vertical-axes have been reported from paleomagnetic studies (Pechersky et al., 1997), including a 76° post-Eocene rotation in the westernmost Aleutians (Bazhenov et al., 1992).

Detroit Seamount located in Figure 1 started accumulating pelagic sediments around 60 Ma (Figure 4). As paleomagnetic data on Late Cretaceous igneous basement rocks of 75-81 Ma reveal a paleolatitude at that time of 34.4° (Dobrovine and Tarduno, 2004), the seamount was at a sub-tropical location when the pelagic cap began accumulating. The Pacific Ocean was then much larger, with Detroit more remote from subduction zones (Scotese et al., 1988) and hence possible arc-sources of internal waves.

Hawaiian Ridge

Subsidence of ocean island chains is more predictable than that of arc island chains so changes in internal tide generation should also be more predictable. According to K-Ar dates compiled by Clague and Dalrymple (1989), volcano ages at the two internal wave generation sites highlighted in Figure 2 are 10-13 Ma. The French Frigate Shoals (FFS) and Kaena Ridge/Kaua'i Channel known to generate internal waves here (Merrifield and Holloway, 2001) are marked with asterisks in the cross-sections (lower-right inset of Figure 1). Prior to 13 Ma, the FFS and other banks east of there would not have existed, a date that is later than when deposition slowed at Site 171 but coincides roughly with the last pelagic deposition on Site 44 (Figure 4).

After vertical motions associated with lithospheric loading by new islands have occurred, subsidence tends to follow the thermal subsidence of the underlying lithosphere after its re-heating during the impact of the mantle plume (Crough, 1983; Detrick and Crough, 1978). Profiles C and D in Figure 2 (lower-right inset) lie 1000-2000 from Kilauea and comprise volcanoes of 12-22 Ma in age (Clague and Dalrymple, 1989). Besides a bank on the far eastern side of C, they show relatively little evidence of shallow sills between edifices. Using the Detrick and Crough (1978) relationship, the amount of subsidence expected over 10 m.y. is a modest ~200 m. Therefore, the westerly Hawaiian Ridge was unlikely to have been a generator of significant internal waves. On Allison Guyot, periods of non-deposition or erosion started just prior to 20 Ma (Figure 4) so we suspect other sources of internal waves or other currents affected it.

Summary

In the subject of paleoceanography, large-scale motions of water in the oceans have been worked out from paleontological, chemical and isotopic changes in pelagic sediments. However, physical movements of bottom waters occur with many higher frequency components and these physical movements are commonly important for modulating particle accumulation or erosion and thus the sedimentary record. In this study, we have examined data on the pelagic caps of seamounts and guyots, which are in shallow water so that chemical dissolution of carbonates is likely to be muted and physical effects on deposition are more likely to dominate. Internal waves provide a significant oscillation in the upper ocean in these areas. Such waves are generated where the barotropic tide passes over shallow ridges, producing oscillations in the pycnocline that travel away from the ridges in beams that are predictable for the modern ocean.

Incidences of non-deposition/erosion and accumulation on guyot summits over the past few million years characterized from scientific drilling and seismic reflection data lie, respectively, on and off the modern beams of internal waves predicted using a global model (Simmons, 2008). Away from boundary currents and sources of strong eddy motions, many of the hiatuses within the pelagic caps of guyots and seamounts were potentially also generated by internal wave motions. The differing termination dates of hiatuses at the different sites suggest they did not have a chemical origin, but rather a physical origin. Their most likely explanation, it seems to us, is plate tectonics. Rotation of the Bonin and Marianas Island arcs recorded in paleomagnetic data has likely changed the orientations of beams from their ridges, though this requires a reconstruction of sill depths to evaluate more fully. The Solomon Islands may have provided sources of

internal waves to the Marshall Islands guyots that can potentially explain hiatuses found there; uplift of several islands documented in the literature combined with plate reconstructions (Mann and Taira, 2004) suggest that shallow sills previously lay orthogonal to Sites 871-873.

Acknowledgements

We thank Bill Ryan and students for their work in revising the absolute chronological data in the legacy DSDP and ODP stratigraphic data used here. We thank Ted Moore and editor Dennis Harry for very helpful reviews. Many of the figures shown here were generated with the GMT software system (Wessel and Smith, 1991). HLS was supported by US National Science Foundation under award number 0968838.

References

- Alford, M. H., 2003, Redistribution of energy available for ocean mixing by long-range propagation of internal waves: *Nature*, v. 423, p. 159-162.
- Alford, M. H., MacKinnon, J. A., Zhao, Z., Pinkel, R., Klymak, J., and Peacock, T., 2007, Internal waves across the Pacific: *Geophys. Res. Lett.*, v. 34, Paper L24601, doi:24610.21029/22007GL031566.
- Alford, M. H., and Zhao, Z., 2007, Global patterns of low-mode internal-wave propagation. Part I: Energy and energy flux: *J. Phys. Oceanogr.*, v. 37, p. 1829-1848.
- Apel, J. R., 1987, *Principles of ocean physics*, New York, Academic Press, 634 pp.
- Barron, J. A., and Keller, G., 1982, Widespread Miocene deep-sea hiatuses: Coincidence with periods of global cooling: *Geology*, v. 10, p. 577-581.

- Bazhenov, M. L., Burtman, V. S., Krezhovskikh, O. A., and Shapiro, M. N., 1992, Paleomagnetism of Paleogene rocks of the Central-East Kamchatka and Komanorsky Islands: tectonic implications: *Tectonophys.*, v. 201, p. 157-173.
- Beaulieu, S. E., 2003, Resuspension of phytodetritus from the sea floor: A laboratory flume study: *Limnol. Oceanogr.*, v. 48, p. 1235-1244.
- Beckmann, A., and Haidvogel, D. B., 1997, A numerical simulation of flow at Fieberling Guyot: *J. Geophys. Res.*, v. 102, p. 5595-5613.
- Berger, W. H., Adelseck, C. G., and Mayer, L. A., 1976, Distribution of carbonate in surface sediments of the Pacific Ocean: *J. Geophys. Res.*, v. 81, no. 15, p. 2617-2627.
- Bijl, P. K., Schouten, S., Sluijs, A., Reichert, G.-J., Zachos, J. C., and Brinkhuis, H., 2009, Early Palaeogene temperature evolution of the southwest Pacific Ocean: *Nature*, v. 461, p. 776-779.
- Black, K. S., Peppe, O. C., and Gust, G., 2003, Erodibility of pelagic carbonate ooze in the northeast Atlantic: *J. Exp. Marine Biol. Ecol.*, v. 285-286, p. 143-163.
- Bograd, S. J., Rabinovich, A. B., LeBlond, P. H., and Shore, J. A., 1997, Observations of seamount-attached eddies in the North Pacific: *J. Geophys. Res.*, v. 102, p. 12441-12456.
- Briden, J. C., Hurley, A. M., and Smith, A. G., 1981, Paleomagnetism and Mesozoic-Cenozoic paleocontinental maps: *J. Geophys. Res.*, v. 86, p. 11631-11656.
- Brink, K. H., 1995, Tidal and lower frequency currents above Fieberling Guyot: *J. Geophys. Res.*, v. 100, p. 10817-10832.
- Cacchione, D. A., and Drake, D. E., 1986, Nepheloid layers and internal waves over continental shelves and slopes: *Geo-Mar. Lett.*, v. 6, p. 147-152.

- Cacchione, D. A., Pratson, L. F., and Ogston, A. S., 2002, The shaping of continental slopes by internal tides: *Science*, v. 296, p. 724-727.
- Cacchione, D. A., Schwab, W. C., Noble, M., and Tate, G., 1988, Internal tides and sediment movement on Horizon Guyot, Mid-Pacific Mountains: *Geo-Mar. Lett.*, v. 8, p. 11-17.
- Chapman, D. C., and Haidwogel, D. B., 1992, Formation of Taylor caps over a tall isolated seamount in a stratified ocean: *Geophys. Astrophys. Fluid Dynamics*, v. 1992, p. 31-65.
- Clague, D. A., and Dalrymple, G. B., 1989, Tectonics, geochronology, and origin of the Hawaiian-Emperor volcanic chain, *in* Winterer, E. L., Hussong, D. M., and Decker, R. W., eds., *The Geology of North America, Volume N: The Eastern Pacific Ocean and Hawaii, Volume DNAG Series, Volume N: Boulder, Colorado, The Geological Society of America*, p. 188-217.
- Codiga, D. L., and Eriksen, C. C., 1997, Observations of low-frequency circulation and amplified subinertial tidal currents at Cobb Seamount: *J. Geophys. Res.*, v. 102, p. 22993-23007.
- Coleman, P. J., 1962, An outline of the geology of Choiseul, British Solomon Islands: *J. Geol. Soc. Aust.*, v. 8, p. 135-157.
- Crook, K. A., and Taylor, B., 1994, Structure and Quaternary tectonic history of the Woodlark Triple Junction region, Solomon Islands: *Marine Geophys. Res.*, v. 16, p. 65-89.
- Crough, S. T., 1983, Hotspot swells: *Ann. Rev. Earth Planet. Sci.*, v. 11, p. 165-193.
- Dekens, P. S., Ravelo, A. C., and McCarthy, M. D., 2007, Warm upwelling regions in the

- Pliocene warm period: *Paleocean.*, v. 22, Article PA3211, doi:3210.1029/2006PA001394.
- Dekens, P. S., Ravelo, A. C., McCarthy, M. D., and Edwards, C. A., 2008, A 5 million year comparison of Mg/Ca and alkenone paleothermometers: *Geochem. Geophys. Geosys.*, v. 9, Article Q10001, doi:10010.11029/12007GC001931.
- Detrick, R. S., and Crough, S. T., 1978, Island subsidence, hot spots, and lithospheric thinning: *J. Geophys. Res.*, v. 83, p. 1236-1244.
- Dobrovine, P. V., and Tarduno, J. A., 2004, Late Cretaceous paleolatitude of the Hawaiian Hot Spot: New paleomagnetic data from Detroit Seamount (ODP Site 883): *Geochemistry, Geophysics, Geosystems*, v. 5, doi:10.1029/2004GC000745.
- Egbert, G. D., and Ray, R. D., 2003, Semi-diurnal and diurnal tidal dissipation from TOPEX/Poseidon altimetry: *Geophys. Res. Lett.*, v. 30, Paper 1907, doi:1910.1029/2003GL017676.
- Egbert, G. D., Ray, R. D., and Bills, B. G., 2004, Numerical modeling of the global semidiurnal tide in the present day and in the last glacial maximum: *J. Geophys. Res.*, v. 109, Art. No. C03003.
- Eriksen, C. C., 1991, Observations of amplified flows atop a large seamount: *J. Geophys. Res.*, v. 96, p. 15227-15236.
- Firing, E., 1987, Deep zonal currents in the central equatorial Pacific: *J. Mar. Res.*, v. 45, p. 791-812.
- Freeland, H., 1994, Ocean circulation at and near Cobb Seamount: *Deep-Sea Res.*, v. 41, p. 1715-1732.
- Gill, A. E., 1982, *Atmosphere-Ocean Dynamics*, New York, Academic Press, International Geophysics Series, vol. 30, 662 p.

- Gradstein, F. M., and Ogg, J. G., 2004, Geological Time Scale 2004 - why, how, and where next!: *Lethaia*, v. 37, p. 175-181.
- Hamilton, E. L., 1979, Sound velocity gradients in marine sediments: *J. Acoust. Soc. Am.*, v. 65, p. 909-922.
- Haston, R., and Fuller, M., 1991, Paleomagnetic data from the Philippine Sea Plate and their tectonic significance: *J. geophys. Res.*, v. 96, p. 6073~6078.
- Hayes, S. P., Toole, J. M., and Mangum, L. J., 1983, Water-mass and transport variability at 110°W in the Equatorial Pacific: *J. Phys. Ocean.*, v. 13, p. 153-168.
- Hilde, T. W. C., Uyeda, S., and Kroenke, L., 1977, Evolution of the western Pacific and its margin: *Tectonophys.*, v. 38, p. 145-165.
- Holloway, P. E., and Merrifield, M. A., 1999, Internal tide generation by seamounts, ridges, and islands: *J. Geophys. Res.*, v. 104, p. 25937-25951.
- Holloway, P. E., and Merrifield, M. A., 2003, On the spring-neap variability and age of the internal tide at the Hawaiian Ridge: *J. Geophys. Res.*, v. 108, Paper 3126, doi:3110.1029/2002JC001486.
- Johnston, T. M. S., and Merrifield, M. A., 2003, Internal tide scattering at seamounts, ridges, and islands: *J. Geophys. Res.*, v. 108, Paper 3180, doi:3110.1029/2002JC001528.
- Joint Panel on Oceanographic Tables and Standards, 1991, Processing of oceanographic station data, Paris, UNESCO, 138 p.
- Kayen, R. E., Schwab, W. C., Lee, H. J., Torresan, M. E., Hein, J. R., Quinerno, P. J., and Levin, L. A., 1989, Morphology of sea-floor landslides on Horizon Guyot: application of steady-state geotechnical analysis: *Deep-Sea Res.*, v. 36, p. 1817-1839.

- Keating, B. H., Kodama, K., and Helsley, C. E., 1983, Paleomagnetic studies of the Bonin and Mariana Island Arcs, *in* Shimozoru, D., and Yokoyama, I., eds., *Arc Volcanism; Physics and Tectonics*: Tokyo, Terra Scientific Publishing, p. 243-259.
- Keller, G., and Barron, J. A., 1983, Paleooceanographic implications of Miocene deep-sea hiatuses: *Geol. Soc. Am. Bull.*, v. 94, p. 590-613.
- Kerr, B. C., Scholl, D. W., and Klemperer, S. L., 2005, Seismic stratigraphy of Detroit Seamount, Hawaiian-Emperor seamount chain: Post-hot-spot shield-building volcanism and deposition of the Meiji drift: *Geochem. Geophys. Geosys.*, v. 6, Paper Q07L10, doi:10.1029/2004GC000705.
- Kodama, K., 1981, A paleomagnetic reconnaissance of the Bonin Islands: *Bull. Earthquake Res. Inst.*, v. 56, p. 347-365.
- Kodama, K., Keating, B. H., and Helsley, C. E., 1983, Paleomagnetism of the Bonin Islands and its tectonic significance: *Tectonophys.*, v. 95, p. 25-42.
- Koizumi, I., Butt, A., Yi Ling, H., and Takayama, T., 1980, Biostratigraphic summary of DSDP Leg 55: Emperor Seamount chain: Initial Reports of the Deep-Sea Drilling Project, V55, Washington (US Government Printing Office), p. 285-288.
- Kunze, E., and Toole, J. M., 1997, Tidally driven vorticity, diurnal shear, and turbulence atop Fieberling Seamount: *J. Phys. Ocean.*, v. 27, p. 2663-2693.
- Larson, E. E., Reynolds, R. L., Ozima, M., Aoki, Y., Kinoshita, H., Zasshu, S., Kawai, N., Nakijima, T., Hirooka, K., Merrill, R., and Levi, S., 1975, Paleomagnetism of Miocene volcanic rocks of Guam and the curvature of the Southern Mariana Island Arc: *Geol. Soc. Am. Bull.*, v. 86, p. 346-350.
- Lavelle, J. W., and Mohn, C., 2010, Motion, commotion, and biophysical connections at

- deep ocean seamounts: *Oceanography*, v. 23, p. 90-103.
- Lear, C. H., Elderfield, H., and Wilson, P. A., 2000, Cenozoic deep-sea temperature and global ice volumes from Mg/Ca in benthic foraminiferal calcite: *Science*, v. 287, p. 269-272.
- Lear, C. H., Mawbey, E. M., and Rosenthal, Y., 2010, Cenozoic benthic foraminiferal Mg/Ca and Li/Ca records: Toward unlocking temperatures and saturation states: *Paleocean.*, v. 25, Paper PA4215, doi:4210.1029/2009PA001880.
- Lear, C. H., and Rosenthal, Y., 2006, Benthic foraminiferal Li/Ca: Insights into Cenozoic seawater carbonate saturation state: *Geology*, v. 34, p. 985-988.
- Leg 55 Scientific Staff, 1980, Leg 55 sediment grain size and carbon/carbonate data: Initial Reports of the Deep-Sea Drilling Project, V55, Washington (US Government Printing Office), p. 861-862.
- Lonsdale, P., Normark, W. R., and Newman, W. A., 1972, Sedimentation and erosion on Horizon Guyot: *Geol. Soc. Am. Bull.*, v. 83, p. 289-316.
- Mann, P., and Taira, A., 2004, Global tectonic significance of the Solomon Islands and Ontong Java Plateau convergent zone: *Tectonophys.*, v. 389, p. 137-190.
- Mann, P., Taylor, F. W., Lagoë, M. B., Quarles, A., and Burr, G., 1998, Accelerating late Quaternary uplift of the New Georgia Island Group (Solomon island arc) in response to subduction of the recently active Woodlark spreading center and Coleman seamount: *Tectonophys.*, v. 295, p. 259-306.
- Mayewski, P. A., Meeker, L. D., Whitlow, S., Tickler, M. S., Morrison, M. C., Bloomfield, P., Bond, G. C., Alley, R. B., Gow, A. J., Grootes, P. M., Meese, D. A., Ram, M., Taylor, K. C., and Wumkes, W., 1994, Changes in atmospheric circulation

- and ocean ice cover over the North Atlantic during the last 41,000 years: *Science*, v. 263, p. 1747-1751.
- McCabe, R., 1984, Implications of paleomagnetic data on the collision related bending of island arcs: *Tectonics*, v. 3, p. 409-428.
- McCave, I. N., 1984, Erosion, transport and deposition of fine-grained marine sediments, *in* Stow, D. A. V., and Piper, D. J. W., eds., *Fine-grained sediments: deep water processes and facies*, *Geol. Soc. Lond. Spec. Pub.* 15, p. 35-69.
- McCave, I. N., and Swift, S. A., 1976, A physical model for the rate of deposition of fine-grained sediments in the deep sea: *Geol. Soc. Am. Bull.*, v. 87, p. 541-546.
- McKenzie, J., Bernoulli, D., and Schlanger, S. O., 1980, Shallow-water carbonate sediments from the Emperor Seamounts: Their diagenesis and paleogeographic significance: *Initial Reports of the Deep-Sea Drilling Project, V55*, Washington (US Government Printing Office), p. 415-455.
- Merrifield, M. A., and Holloway, P. E., 2001, Model estimates of M_2 internal tide energetics at the Hawaiian Ridge: *J. Geophys. Res.*, v. 107, Paper 3179, doi:3110.1029/2001JC000996.
- Merrifield, M. A., Holloway, P. E., and Johnston, T. M. S., 2001, The generation of internal tides at the Hawaiian Ridge: *Geophys. Res. Lett.*, v. 28, p. 559-562.
- Meschede, M., and Frisch, W., 1998, A plate-tectonic model for the Mesozoic and Early Cenozoic history of the Caribbean plate: *Tectonophys.*, v. 196, p. 269-291.
- Mitchell, N. C., 1995, Diffusion transport model for pelagic sediments on the Mid-Atlantic Ridge: *J. Geophys. Res.*, v. 100, no. B10, p. 19,991-920,009.
- Mitchell, N. C., 1998, Modeling Cenozoic sedimentation in the central equatorial Pacific

- and implications for true polar wander: *J. Geophys. Res.*, v. 103, p. 17749-17766.
- Mitchell, N. C., and Huthnance, J. M., 2007, Oceanographic currents and the convexity of the uppermost continental slope: *J. Sediment. Res.*, v. 78, p. 29-44.
- Mitchell, N. C., and Huthnance, J. M., 2013, Geomorphological and geochemical evidence (^{230}Th anomalies) for cross-equatorial currents in the central Pacific: *Deep-Sea Res. I.*, v. 78, p. 24-41.
- Mohn, C., White, M., Bashmachnikov, I., Jose, F., and Pelegrí, J. L., 2009, Dynamics at an elongated, intermediate depth seamount in the North Atlantic (Sedlo Seamount, $40^{\circ}20'\text{N}$, $26^{\circ}40'\text{W}$): *Deep-Sea Res. II*, v. 56, p. 2582-2592.
- Moore, T. C., 2013, Erosion and reworking of Pacific sediments near the Eocene-Oligocene boundary: *Paleocean.*, v. 28, p. 263–273, doi:210.1002/palo.20027.
- Moore, T. C., van Andel, T. H., Sancetta, C., and Pisias, N., 1978, Cenozoic hiatuses in pelagic sediments: *micropaleontology*, v. 24, p. 113-138.
- Mouriño, B., Fernández, E., Serret, P., Harbour, D., and Sinha, B., 2001, Variability and seasonality of physical and biological fields at the Great Meteor Tablemount (subtropical NE Atlantic): *Oceanol. Acta*, v. 24, p. 167-185.
- Musgrave, R., 1990, Paleomagnetism and tectonics of Malaita, Solomon Islands: *Tectonics*, v. 9, p. 735-759.
- Noble, M., Cacchione, D. A., and Schwab, W. C., 1988, Observations of strong mid-Pacific internal tides above Horizon Guyot: *J. Phys. Oceanogr.*, v. 18, p. 1300-1306.
- Odd, N. V. M., and Owen, M. W., 1972, A two-layer model of mud transport in the Thames Estuary: *Inst. Civil Engineers Proc.*, suppl. 9, p. 175 -205.
- Pälike, H., et al., 2012, A Cenozoic record of the equatorial Pacific carbonate compensation

- depth: *Nature*, v. 488, p. 609-615.
- Pearson, P. N., 1995, Planktonic foraminifer biostratigraphy and the development of pelagic caps on guyots in the Marshall Island group, *in* Haggerty, J. A., Premoli Silva, L., Rack, F., and McNutt, M. K., eds., *Proceedings of the Ocean Drilling Program, Scientific Results, Volume 144*: College Station, Texas, Ocean Drilling Program, p. 21-59.
- Pearson, P. N., Ditchfield, P., and Shackleton, N. J., 2002, Palaeoclimatology - Tropical temperatures in greenhouse episodes - Reply: *Nature*, v. 419, p. 898.
- Pearson, P. N., Ditchfield, P. W., Singano, J., Harcourt-Brown, K. G., Nicholas, C. J., Olsson, R. K., Shackleton, N. J., and Hall, M. A., 2001, Warm tropical sea surface temperatures in the Late Cretaceous and Eocene epochs: *Nature*, v. 413, p. 481-487.
- Pearson, P. N., van Dongen, B. E., Nicholas, C. J., Pancost, R. D., Schouten, S., Singano, J. M., and Wade, B. S., 2007, Stable warm climate through the Eocene Epoch: *Geology*, v. 35, p. 211-214.
- Pechersky, D. M., Levashova, N. M., Shapiro, M. N., Bazhenov, M. L., and Sharonova, Z. V., 1997, Palaeomagnetism of Palaeogene volcanic series of the Kamchatsky Mys Peninsula, East Kamchatka: the motion of an active island arc: *Tectonophys.*, v. 273, p. 219-237.
- Peterson, L. C., and Prell, W. L., 1985, Carbonate dissolution in recent sediments of the Eastern Equatorial Indian Ocean: preservation patterns and carbonate loss above the lysocline: *Mar. Geol.*, v. 64, p. 259-290.
- Peterson, M. N. A., 1966, Calcite: rates of dissolution in a vertical profile in the central Pacific: *Science*, v. 154, p. 1542-1544.

- Petterson, M. G., Babbs, T., Neal, C. R., Mahoney, J. J., Saunders, A. D., Duncan, R. A., Tolia, D., Magu, R., Qopoto, C., Mahoa, H., and Natogga, D., 1999, Geological–tectonic framework of Solomon Islands, SW Pacific: crustal accretion and growth within an intra-oceanic setting: *Tectonophys.*, v. 301, p. 35-60.
- Premoli Silva, L., Haggerty, J., Rack, F., et al., 1993, Proc. Ocean Drill. Program, Init. Repts. Vol 144, College Station, TX, Ocean Drill. Program.
- Ray, R. D., and Cartwright, D. E., 2001, Estimates of internal tide energy fluxes from Topex/Poseidon altimetry: Central North Pacific: *Geophys. Res. Lett.*, v. 28, p. 1259-1262.
- Ryan, W. B. F., Carbotte, S. M., Coplan, J. O., O'Hara, S., Melkonian, A., Arko, R., Wiessel, R. A., Ferrini, V., Goodwillie, A., Nitsche, F., Bonczkowski, J., and Zemsky, R., 2009, Global multi-resolution topography synthesis: *Geochem. Geophys. Geosys.*, v. 10, Paper Q03014.
- Schuth, S., Münker, C., König, S., Qopoto, C., Basi, S., Garbe-Schönberg, D., and Ballhaus, C., 2009, Petrogenesis of Lavas along the Solomon Island Arc, SW Pacific: Coupling of Compositional Variations and Subduction Zone Geometry: *J. Petrol.*, v. 50, p. 781-811.
- Schwab, W. C., Lee, H. J., Kayen, R. E., Quintero, P. J., and Tate, G. B., 1988, Erosion and slope instability on Horizon Guyot, Mid-Pacific Mountains: *Geo-Mar. Lett.*, v. 8, p. 1-10.
- Scotese, C. R., Gahagan, L. M., and Larson, R. L., 1988, Plate tectonic reconstructions of the Cretaceous and Cenozoic ocean basins: *Tectonophys.*, v. 155, p. 27-48.
- Shipboard Scientific Party, 1971, Site 44, *in* Heezen, B. C., et al., eds., Initial Reports of

the Deep Sea Drilling Project, Volume 6: Washington, DC, U.S. Govt. Printing Office, p. 17-39.

Shipboard Scientific Party, 1973, Tertiary pelagic ooze on Ita Maitai Guyot, equatorial Pacific: DSDP Sites 200 and 201, *in* Heezen, B. C., MacGregor, I. D., et al., eds., Init. Repts. DSDP Vol. 20, Volume 20: Washington, D.C., US Govt. Printing Office, p. 87-96.

Shipboard Scientific Party, 1977a, Site 430: Ojin Seamount: Initial Reports of the Deep-Sea Drilling Project, V55, Washington (US Government Printing Office), v. 55, p. 45-76.

Shipboard Scientific Party, 1977b, Site 433: Suiko Seamount: Initial Reports of the Deep-Sea Drilling Project, V55, Washington (US Government Printing Office), v. 55, p. 127-282.

Shipboard Scientific Party, 1993a, Site 865, *in* Sager, W. W., Winterer, E. L., and Firth, J. V., eds., Proc. Ocean Drill. Program, Init. Repts., Volume 143: College Station, Texas, Ocean Drilling Program, p. 111-181.

Shipboard Scientific Party, 1993b, Site 866, *in* Sager, W. W., Winterer, E. L., and Firth, J. V., eds., Proc. Ocean Drill. Program, Init. Repts., Volume 143: College Station, Texas, Ocean Drilling Program, p. 181-271.

Shipboard Scientific Party, 1993c, Site 878, *in* Premoli Silva, L., Haggerty, J., and Rack, F., eds., Proc. Ocean Drill. Program, Init. Repts., Volume 144: College Station, Texas, Ocean Drilling Program, p. 331-412.

Simmons, H. L., 2008, Spectral modification and geographic distribution of the semi-diurnal internal tide: Ocean Modelling, v. 21, p. 126-138.

- Smith, W. H. F., and Sandwell, D. T., 1997, Global sea floor topography from satellite altimetry and ship soundings: *Science*, v. 277, p. 1956-1962.
- Southard, J. B., Young, R. A., and Hollister, C. D., 1971, Experimental erosion of calcareous ooze: *J. Geophys. Res.*, v. 76, p. 5903-5909.
- Stewart, D. R. M., Pearson, P. N., Ditchfield, P. W., and Singano, J. M., 2004, Miocene tropical Indian Ocean temperatures: evidence from three exceptionally preserved foraminiferal assemblages from Tanzania: *J. African Earth Sci.*, v. 40, p. 173-190.
- Taft, B. A., Hickey, B. M., Wunsch, C., and D. J. Baker, J., 1974, Equatorial undercurrent and deeper flows in the central Pacific: *Deep-Sea Res.*, v. 21, p. 403-430.
- Taylor, G. I., 1923, Experiments on the motion of solid bodies in rotating fluid: *Proceedings of the Royal Society of London A*, v. 104, p. 213-218.
- Thiede, J., 1981, Reworking in upper Mesozoic and Cenozoic central Pacific deep sea sediments: *Nature*, v. 289, p. 667-670.
- Thompson, R. B., and Hackman, B. D., 1969, Geological Notes on Areas Visited by the Royal Society Expedition to the British Solomon Islands: *Phil. Trans Roy. Soc. Ser. B*, v. 255, p. 189-202.
- Thomsen, L., and Gust, G., 2000, Sediment erosion thresholds and characteristics of resuspended aggregates on the western European continental margin: *Deep-Sea Res. I.*, v. 47, p. 1881-1897.
- Turnewitsch, R., Falahat, S., Nycander, J., Dale, A., Scott, R. B., and Furnival, D., 2013, Deep-sea fluid and sediment dynamics - influence of hill- to seamount-scale seafloor topography: *Earth-Science Rev.*, v. 127, p. 203-241.
- Turnewitsch, R., Reyss, J.-L., Chapman, D. C., Thomson, J., and Lampitt, R. S., 2004,

- Evidence of a sedimentary fingerprint of an asymmetric flow field surrounding a short seamount: *Earth and Planet. Sci. Letts.*, v. 222, p. 1023-1036.
- Ujiié, H., 1984, A Middle Miocene hiatus in the Pacific region: its stratigraphic and paleoceanographic significance: *Paleogeogr., Paleoclimat., Palaeoecol.*, v. 46, p. 143-164.
- Uyeda, S., and Miyahiro, A., 1974, Plate tectonics and the Japanese Islands: a synthesis: *Geol. Soc. Am. Bull.*, v. 85, p. 1159-1170.
- van Waasbergen, R. J., and Winterer, E. L., 1993, The Mesozoic Pacific: Geology, Tectonics, and Volcanism. *Geophys. Monogr. 77*, in Pringle, M. S., Sager, W. W., Sliter, W. V., and Stein, S., eds., Volume 77: Washington, D.C., Am. Geophys. Union, p. 335-366.
- Verron, J., and Le Provost, C., 1985, A numerical study of quasi-geostrophic flow over isolated topography: *J. Fluid Mech.*, v. 154, p. 231-252.
- Wara, M. W., Ravelo, A. C., and Delaney, M. L., 2005, Permanent El Niño-like conditions during the Pliocene warm period: *Science*, v. 309, p. 758-761.
- Watkins, D. K., Pearson, P. N., Erba, E., Rack, F. R., Silva, I. P., Bohrmann, H. W., Fenner, J., and Hobbs, P. R. N., 1995, Stratigraphy and sediment accumulation patterns of the Upper Cenozoic pelagic carbonate caps of guyots in the Northwestern Pacific Ocean, in Haggerty, J. A., Premoli Silva, L., Rack, F., and McNutt, M. K., eds., *Proceedings of the Ocean Drilling Program, Scientific Results, Volume 144*: College Station, Texas, Ocean Drilling Program, p. 675-689.
- Wessel, P., and Smith, W. H. F., 1991, Free software helps map and display data: *Eos, Transactions, American Geophysical Union*, v. 72, p. 441.

- Winterer, E. L., and Sager, W. W., 1995, Synthesis of drilling results from the mid-Pacific mountains : regional context and implications, *in* Winter, E. L., Sager, W. W., Firth, J. V. and Sinton, J. M., eds., Proceedings of the Ocean Drilling Program, Scientific Results, Volume 143: College Station, Texas, p. 497-535.
- Winterer, E. L., van Waasbergen, R., Mammerickx, J., and Stuart, S., 1995, Karst morphology and diagenesis of the top of Albian limestone platforms, Mid-Pacific Mountains, *in* Winterer, E. L., Sager, W. W., Firth, J. V., and Sinton, J. M., eds., Proc. Ocean Drill. Program, Sci. Results, Volume 143: College Station, TX (Ocean Drilling Program), p. 433-470.
- Wunsch, C., 1969, Progressive internal waves on slopes: *J. Fluid Mech.*, v. 35, p. 131-144.
- Zachos, J. C., Arthur, M. A., Bralower, T. J., and Spero, H. J., 2002, Palaeoclimatology: Tropical temperatures in greenhouse episodes: *Nature*, v. 419, p. 879-898.
- Zachos, J. C., Dickens, G. R., and Zeebe, R. E., 2008, An early Cenozoic perspective on greenhouse warming and carbon-cycle dynamics: *Nature*, v. 451, p. 279-283.
- Zhang, X., and Boyer, D. L., 1991, Current deflections in the vicinity of multiple seamounts: *J. Phys. Ocean.*, v. 21, p. 1122-1138.
- Zhao, Z., Alford, M. H., MacKinnon, J. A., and Pinkel, R., 2010, Long-range propagation of the semidiurnal internal tide from the Hawaiian Ridge: *J. Phys. Oceanogr.*, v. 40, p. 713-736.

Figures

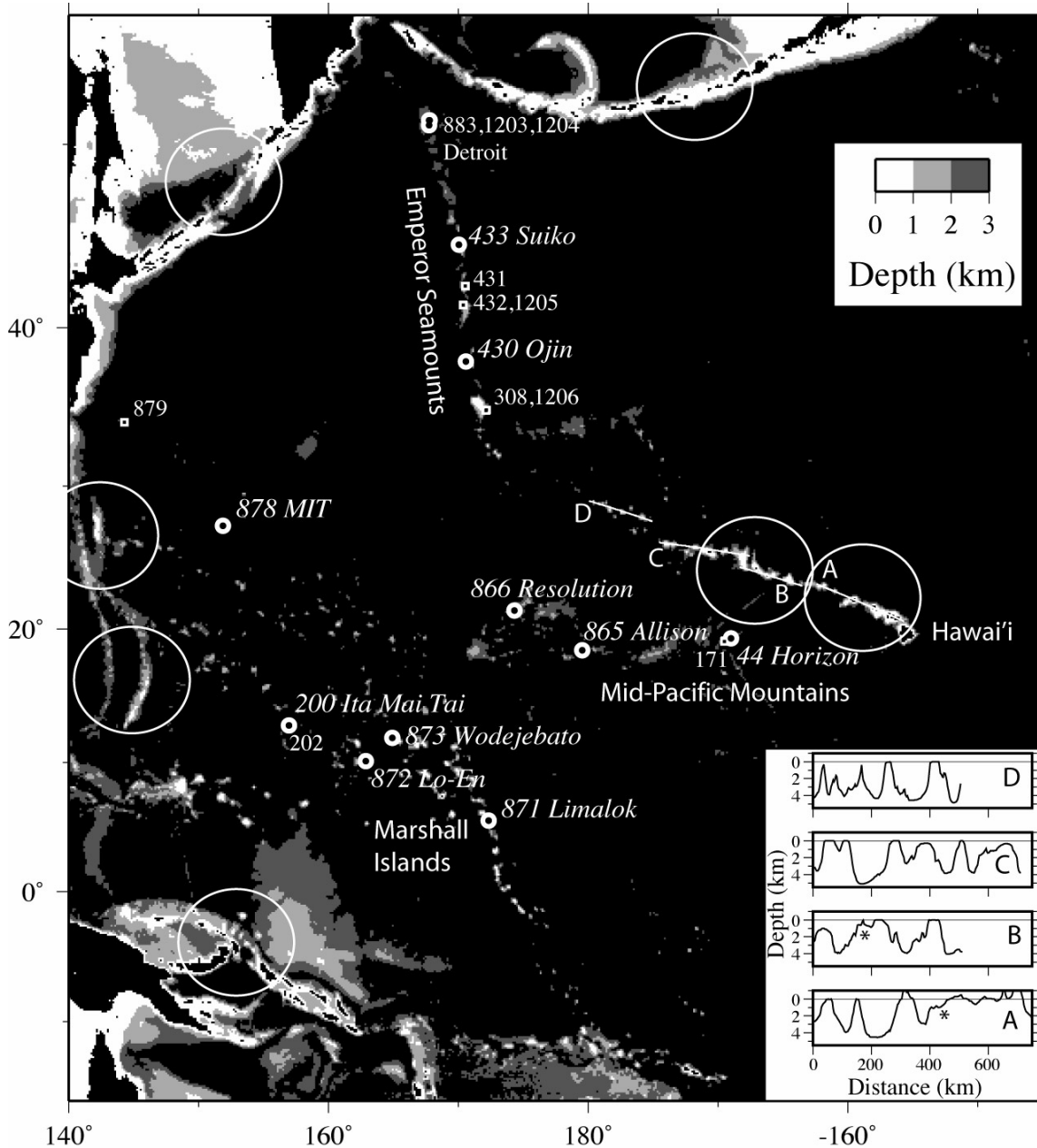


Figure 1. Bathymetry of the central-west Pacific Ocean, highlighting 0-3 km depths relevant to internal wave generation. Black areas represent depths >3 km and land areas (islands outlined in white). Numbers are scientific drilling sites; those with large white circles are guyot or seamount sites with superior seismic and sample data for assessing internal wave effects. Large circles are some sites of internal wave generation (Figure 2).

Lower-right inset: three bathymetry profiles corresponding to lines A, B, C and D marked along the Hawaiian island-seamount chain.

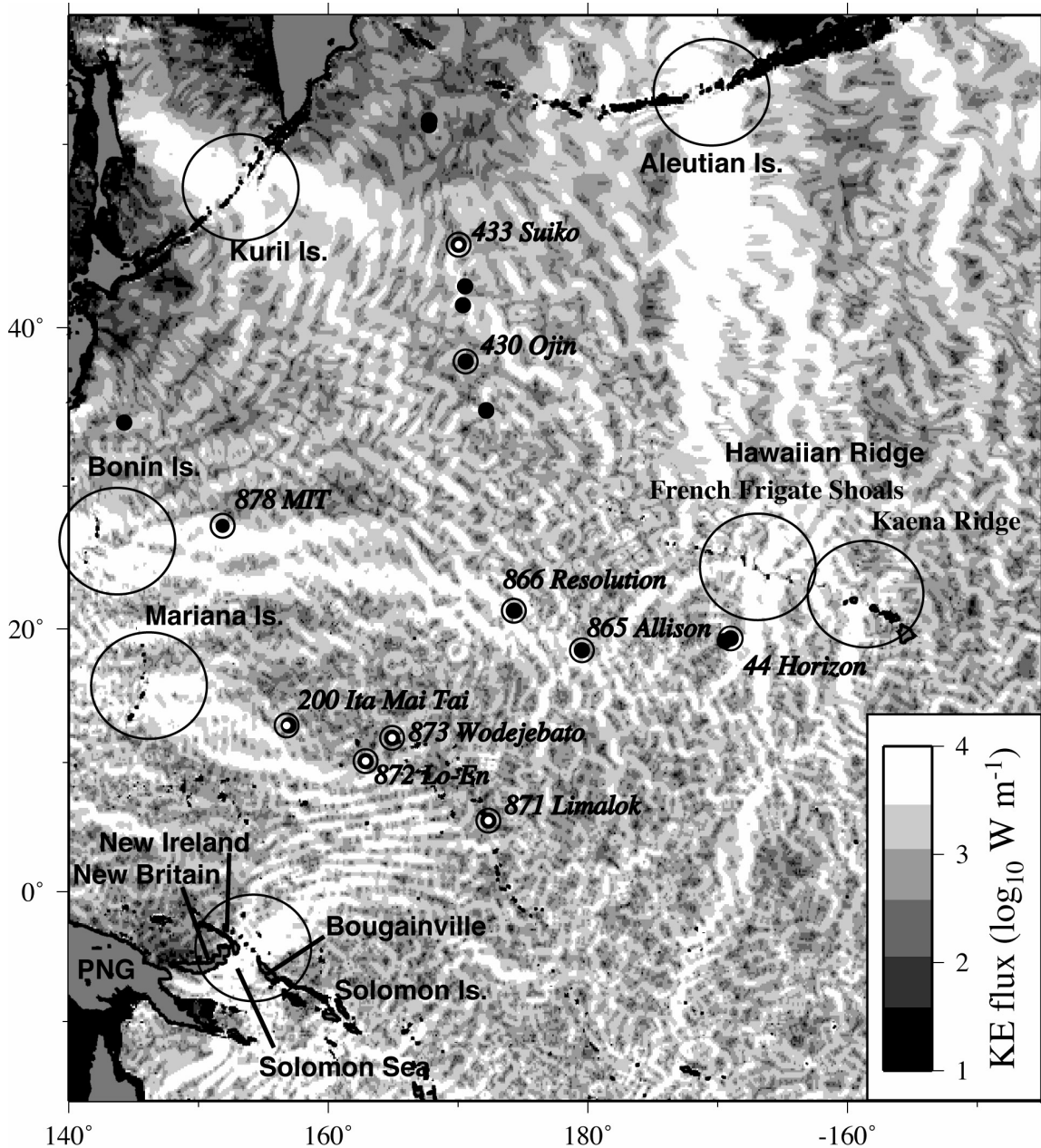


Figure 2. Map of the Pacific internal tidal wave field (Simmons, 2008). White represents high kinetic (KE) energy flux of propagating internal waves, in practice areas of probable larger amplitude waves and greater oscillating current components due to them. Large

circles highlight locations where major beams of internal wave energy are generated. Superimposed are locations of the scientific drilling sites. Ringed solid circles are sites classified as presently eroding or non-depositing and ringed open circles are sites classified as areas where pelagic sediments are presently depositing. Solid circles without rings are other drill sites where data are shown in Figure 4 though information was considered insufficient for classification.

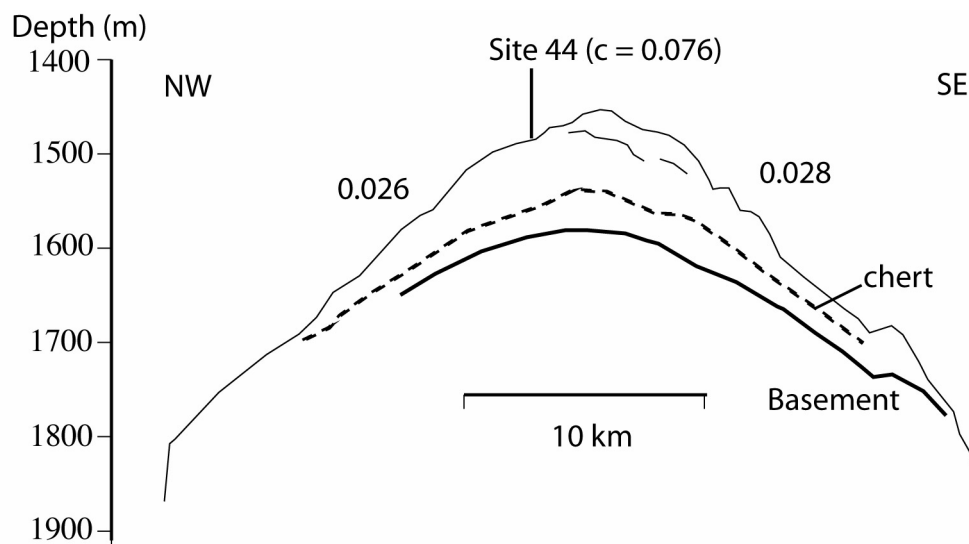


Figure 3. Interpretation of seismic reflection record over Horizon Guyot through DSDP Site 44 adapted from Shipboard Scientific Party (1971). Numbers above profile are seabed gradients (m/m) of the sides of the pelagic cap. Value 'c' next to site number is the local semi-diurnal wave characteristic gradient computed for the site depth.

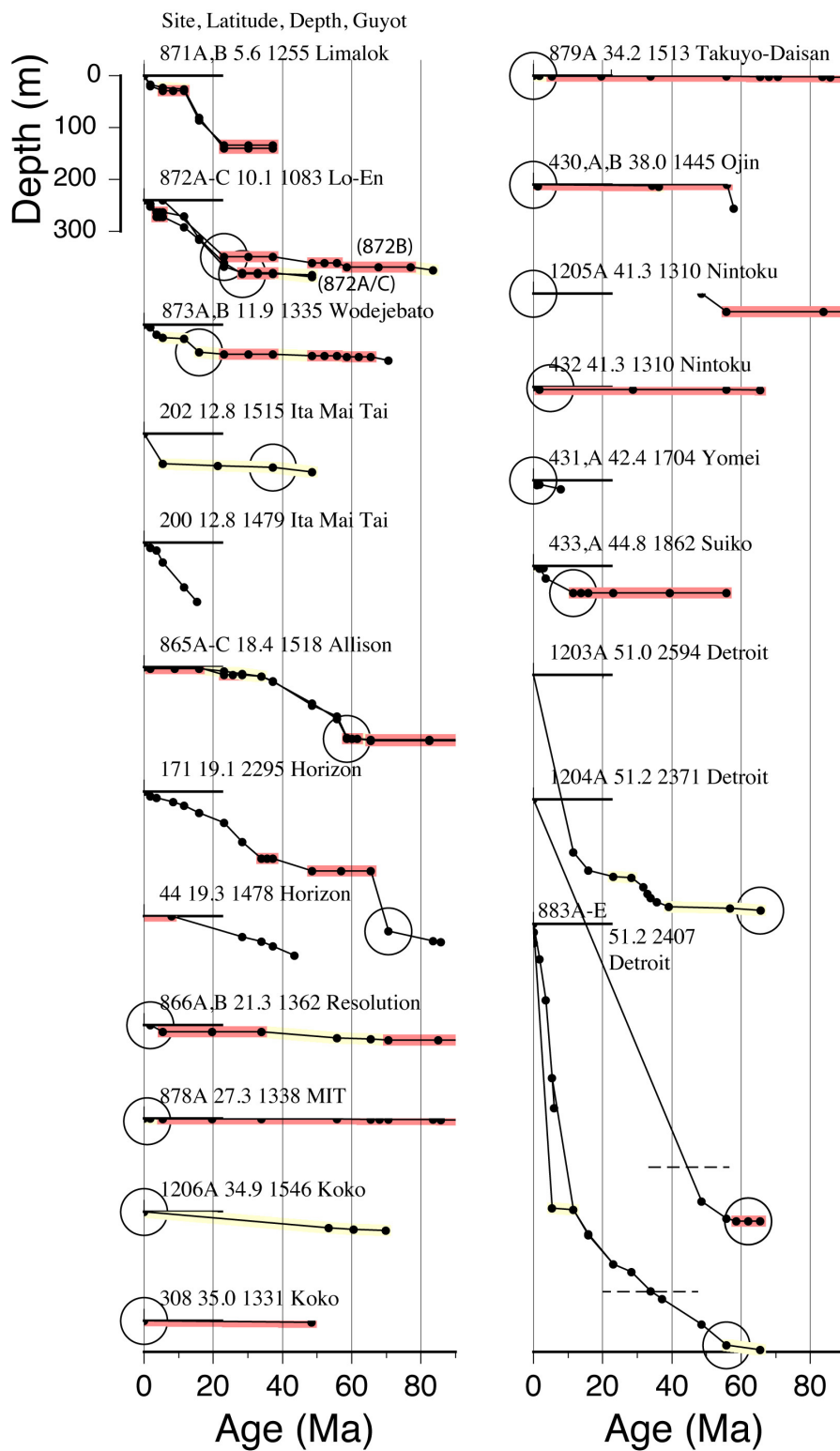


Figure 4. Variation in stratigraphic age with depth below seabed for pelagic caps on Pacific guyots and seamounts drilled during DSDP and ODP. Sites are arranged in latitude order, starting (upper-left) from near the equator. The scientific drilling data have been updated to modern stratigraphic ages provided within the GeoMapApp database (WBF Ryan, pers. comm., 2009; Gradstein and Ogg, 2004). Red and yellow represent sections with sedimentation rates less than 0.1 and 1.0 m m.y.^{-1} , respectively. Annotation above each profile gives the drill site number, latitude (degrees north), water depth (m) and guyot or seamount name. Dashed lines in the last two Detroit Seamount profiles represent the “B” reflector identified as the base of the Meiji Drift (Kerr et al., 2005) (pelagic stage is below this). Circles mark interpreted start of pelagic sediment accumulation; dated sediments below this are commonly platform carbonates or sediments within volcanic sequences.

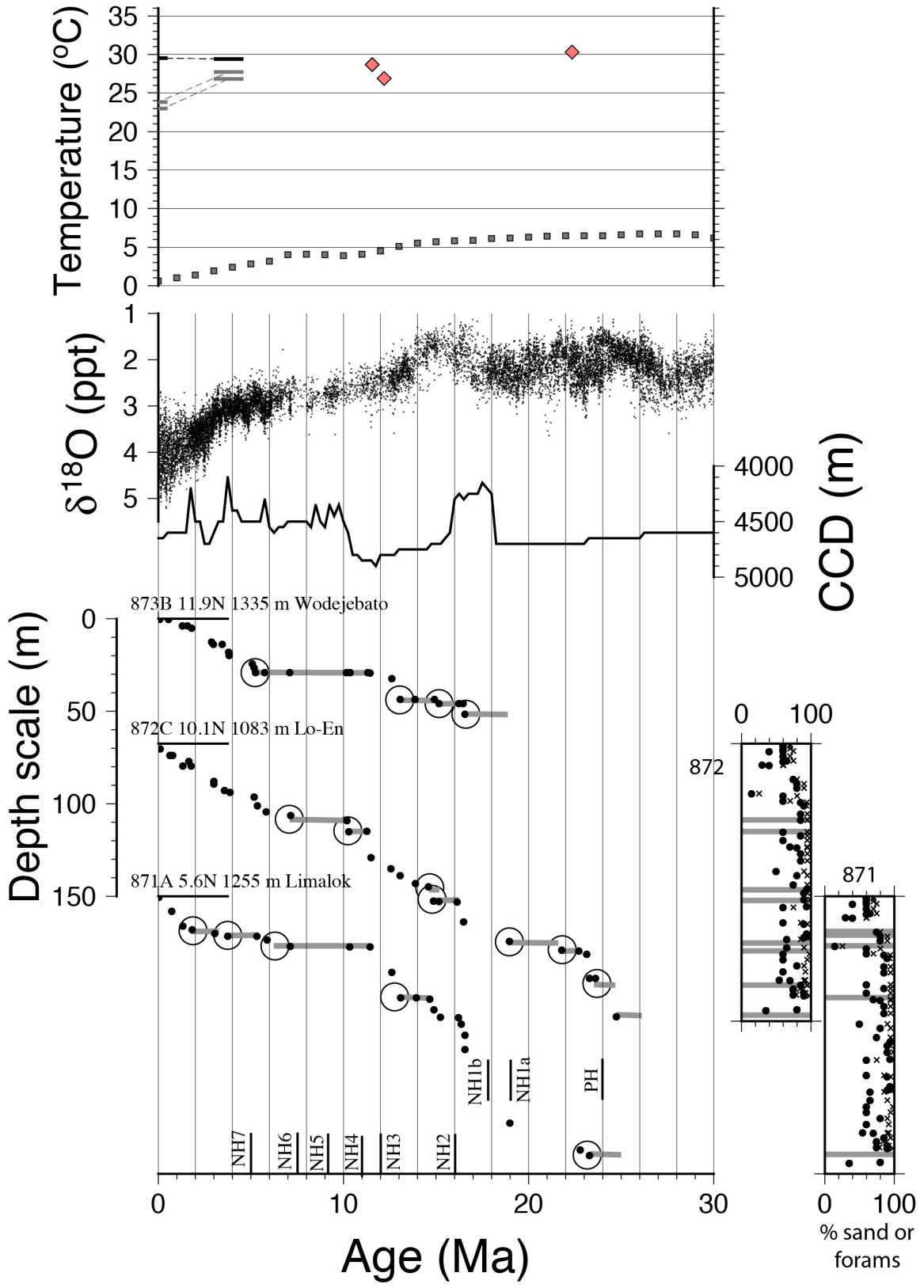


Figure 5. Lower three graphs show the sediment age variation with depth below seabed for three sites on guyot pelagic caps among the Marshall Islands. Points are individual age constraints from the biostratigraphy of Pearson (1995). Grey bars represent his interpretations of the sediment depths of hiatuses (points within bars may represent persistently slow sedimentation). Circles mark the oldest biostratigraphic age of sediment immediately overlying each hiatus. Solid black bar marks the seabed at each site. Vertical bars with annotation NH7, etc, are the Neogene hiatuses and one Paleogene hiatus identified by Keller and Barron (1983) converted to the stratigraphic timescale adopted in the GeoMapApp database (bars located at approximate centers of each missing interval). To the right of these graphs are shown % sand (solid circles) and % of biogenic particles classed as foraminifers (x-symbols) from the smear slide analyses for Sites 871 and 872 (grey bars mark the hiatuses of Pearson (1995)). Also shown are estimated Cenozoic CCD (Pälike et al., 2012), stack of benthic foraminifera $\delta^{18}\text{O}$ obtained from DSDP and ODP cores (Zachos et al., 2008) and ocean paleotemperatures from Figure 6. Note the $\delta^{18}\text{O}$ data are inverted so that isotopic shifts associated with sea level lowerings are down the page.

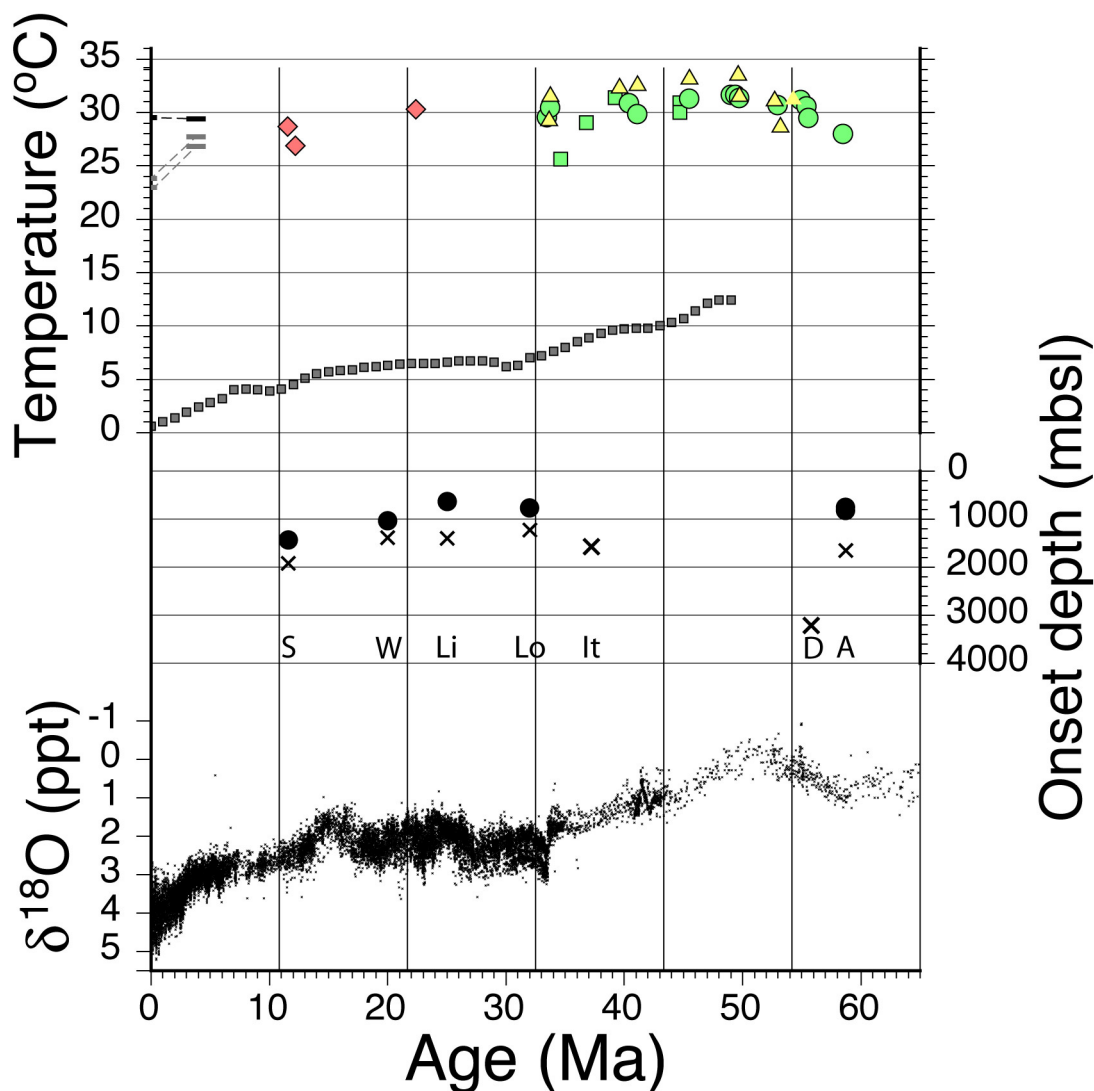


Figure 6. Upper graph shows estimates of tropical ocean paleo-temperatures. Grey squares are deep ocean temperatures estimated from Mg/Ca ratios of benthic foraminifera (Lear et al., 2000). Colored symbols represent maximum temperatures of pelagic foraminifera from Tanzania estimated by oxygen isotopes and TEX_{86} analyses: red diamonds, yellow triangles, green circles and green squares correspond with Stewart et al. (2004), Pearson et al. (2007, TEX_{86}), Pearson et al. (2007, O-18) and Pearson et al. (2001), respectively (TEX_{86} is an index comprising ratios of different 86-carbon organic compounds, which is used as a paleotemperature proxy). In upper-left, grey-filled

symbols are alkenone-based paleotemperature data of Dekens et al. (2008) from the eastern equatorial Pacific (Site 847) and black-filled symbols are Mg/Ca-based paleotemperature data of Wara et al. (2005) from the western equatorial Pacific (Site 806) taken from Dekens et al. (2007).

Middle graph shows the reconstructed depths below sea level at which pelagic accumulation on guyot caps began and their stratigraphic ages (solid circles) and modern depths of this transition ('x' symbols). Only sites drilled away from summit margins are included. Annotation below symbols represents Suiko (S, Site 433), Wodejebato (W, 873), Limalok (Li, 871), Lo-En (Lo, 872), Ita Mai Tai (It, 202), Detroit (D, 883 and 1204) and Allison (A, 865).

Lower-most graph shows the benthic foraminifera $\delta^{18}\text{O}$ stack (Zachos et al., 2008).

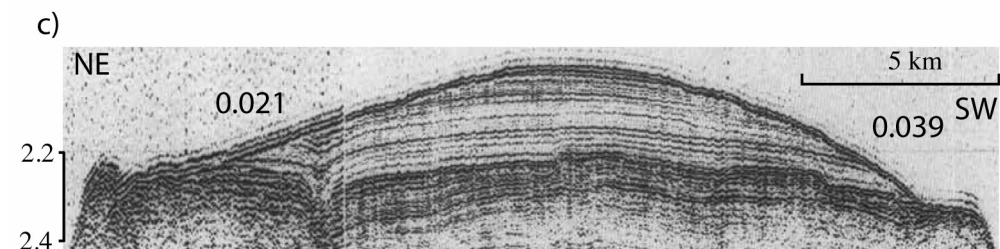
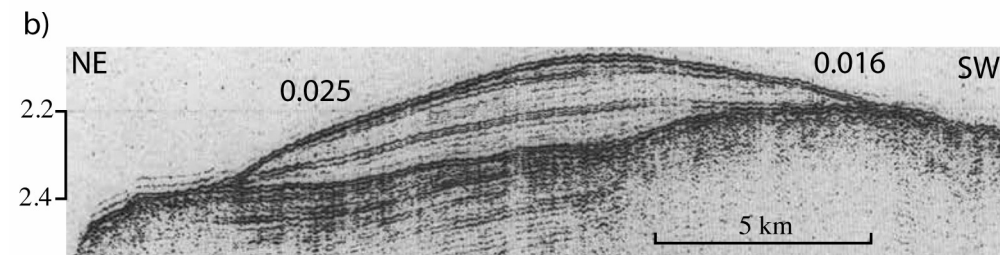
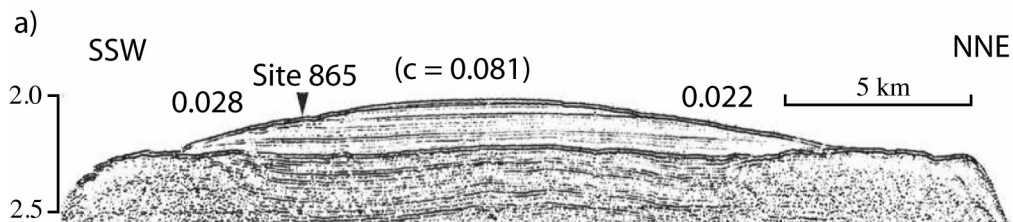


Figure 7. Seismic reflection records crossing the pelagic cap of Allison guyot adapted from (a) Figure 16 of Winterer and Sager (1995) and (b and c) Figures 6 and 7 of Winterer et al. (1995). Vertical axis scales (left) are in seismic two-way travel time (seconds). Numbers above profile are seabed gradients (m/m) of the sides of the pelagic cap. ODP Site 865 is located in (a). Vertical exaggerations of seabed profiles are 6.7:1 (a), 13:1 (b) and 13:1 (c). Value c above (a) is the local internal wave critical gradient.

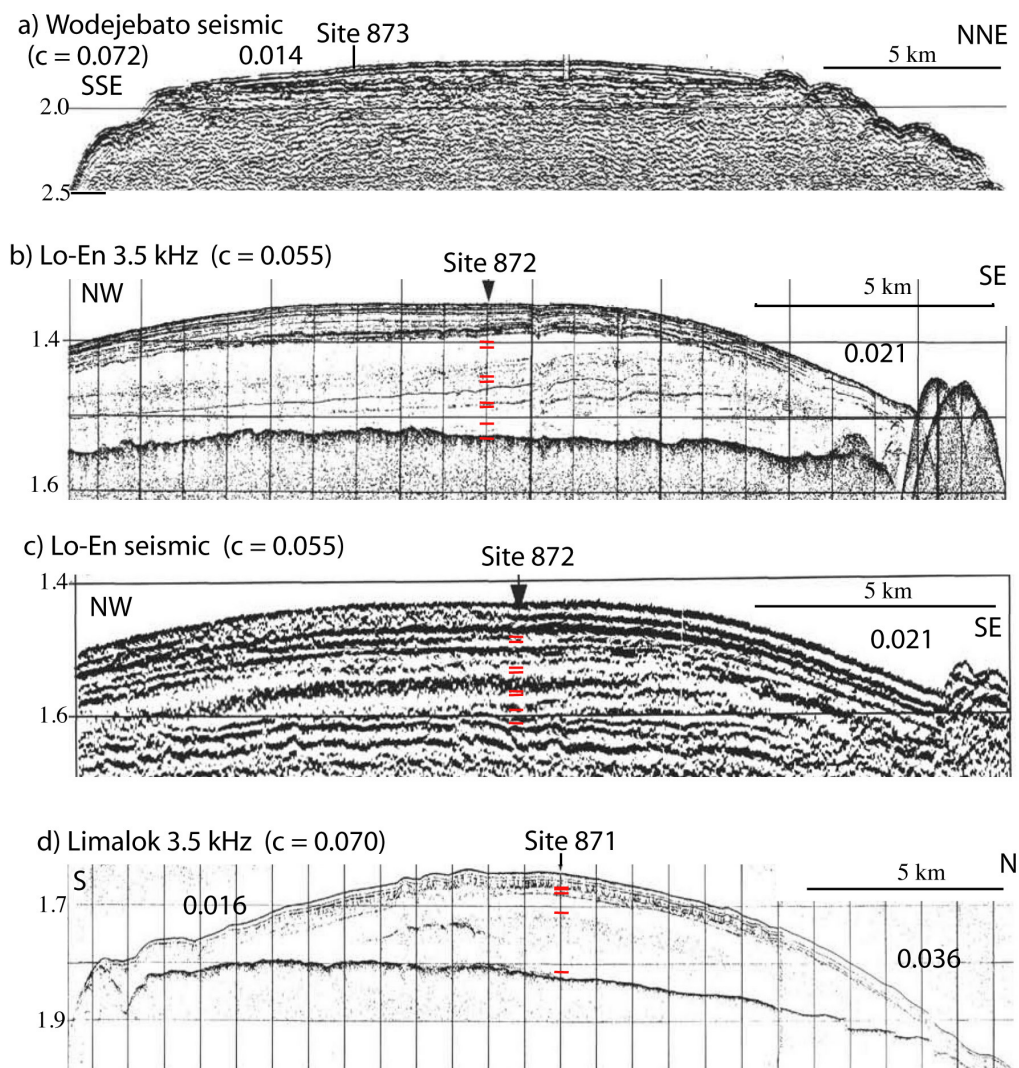


Figure 8. Seismic reflection and 3.5 kHz profiler records (Premoli Silva et al., 1993) crossing the pelagic caps of Lo-En, Limalok and Wodejebato guyots, as Figure 7. Red

marks at drill sites in (b)-(d) locate the hiatuses in the ODP cores from Figure 5 at seismic two-way time calculated assuming a 1633 m s^{-1} seismic velocity (Hamilton, 1979).

Numbers above the sides of the pelagic caps are seabed gradients (m/m) calculated from the records. Profiles (b) and (c) were collected along the same survey line.

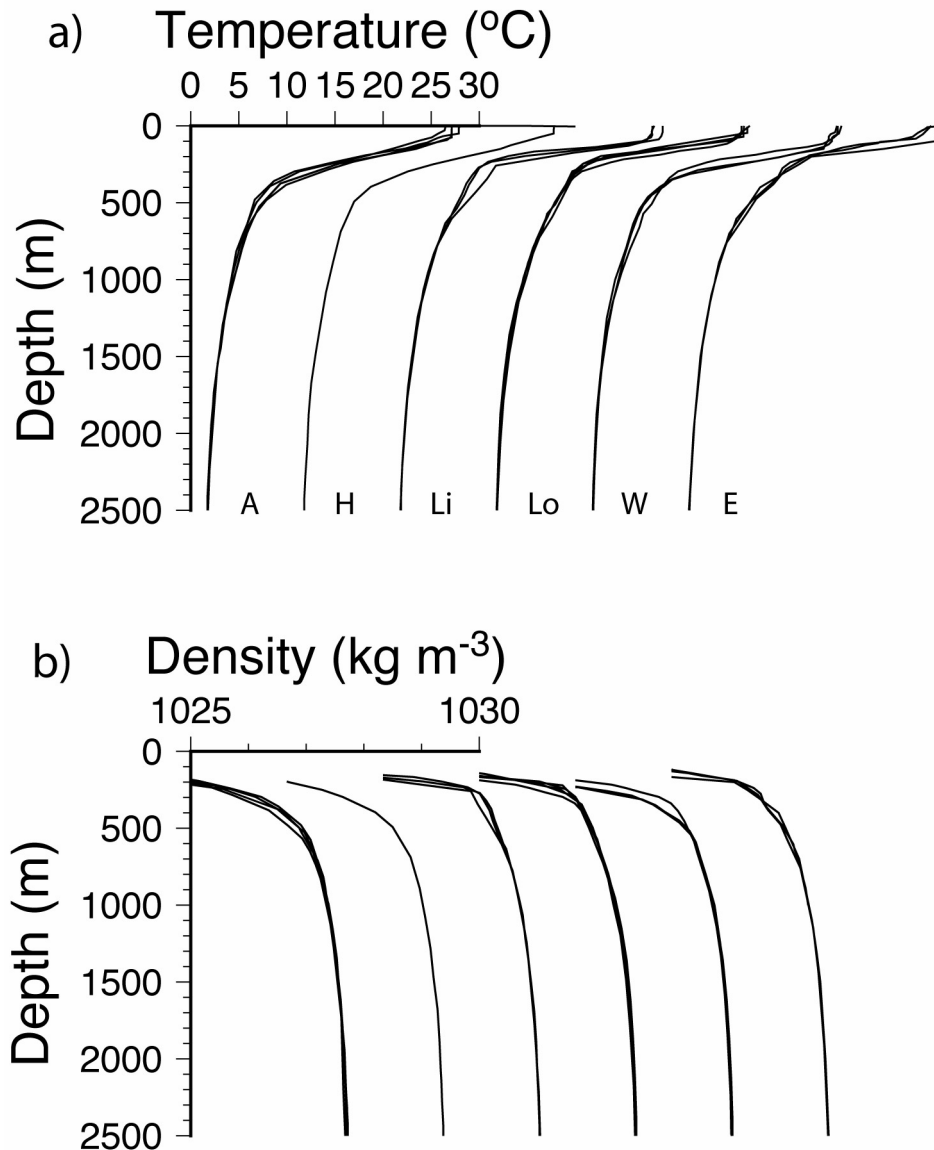


Figure 9. (a) Temperature- and (b) potential density profiles computed from ocean conductivity-temperature-depth measurements at the various guyot sites and on the

Pacific equator. Potential densities were computed using the procedure in Joint Panel on Oceanographic Tables and Standards (1991). A, H, Li, Lo, W and E correspond to Allison, Horizon, Limalok, Lo-En, Wodejebato and equatorial sites, respectively. Graphs are offset laterally to allow interpretation (temperature and density values marked above graphs correspond to the Allison data).

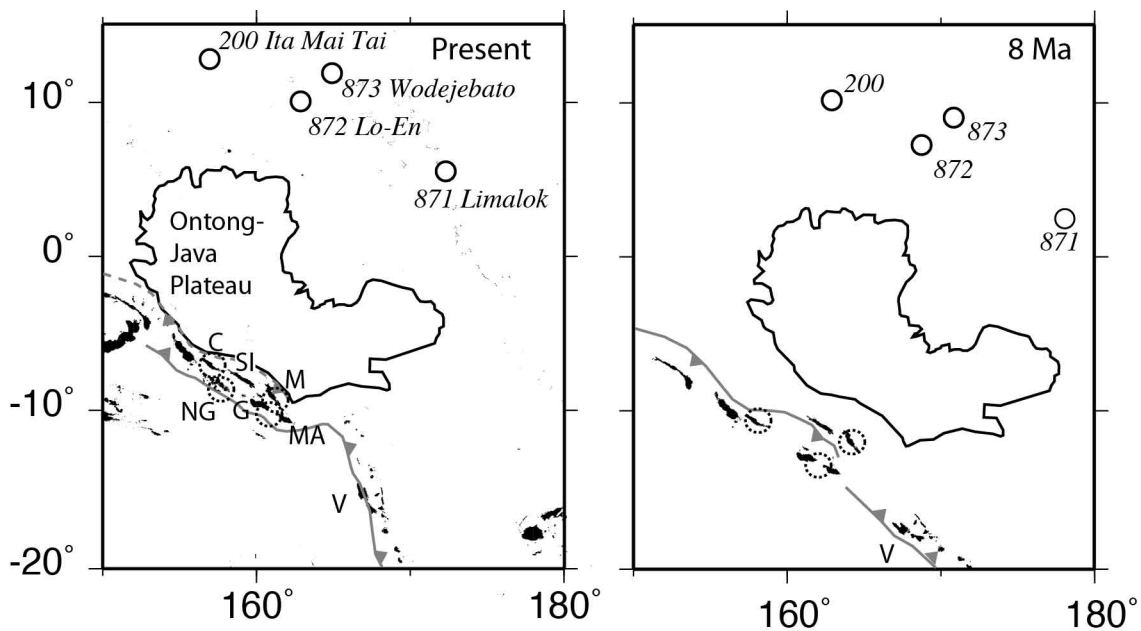


Figure 10. Relationship of the Marshall Islands drill sites to the Solomon Islands at the present day and at 8 Ma, based on plate-tectonic reconstructions of Mann and Taira (2004). The following islands and island groups are annotated: C, Choiseul; NG, New Georgia Island Group; G, Guadalcanal; MA, Makira; V, Vanuatu. Dotted circles are previously submerged islands or deeper seaways discussed in the text as potential earlier sources of internal tidal waves. Grey lines represent the subduction zones with barbs marking the over-riding plate.